NUREG/CR-1412
ANL/ES-88

NUREG/CR-1412
ANL/ES-88

75/1412

SYSTEMS FOR CONTINUOUS MEASUREMENT OF AIRBORNE RADON-222 CONCENTRATION AND WORKING LEVEL

by

Michael H. Momeni, Albin J. Zielen,
James E. Miranda, Jr., Norbert D. Kretz,
and Walter E. Kisieleski

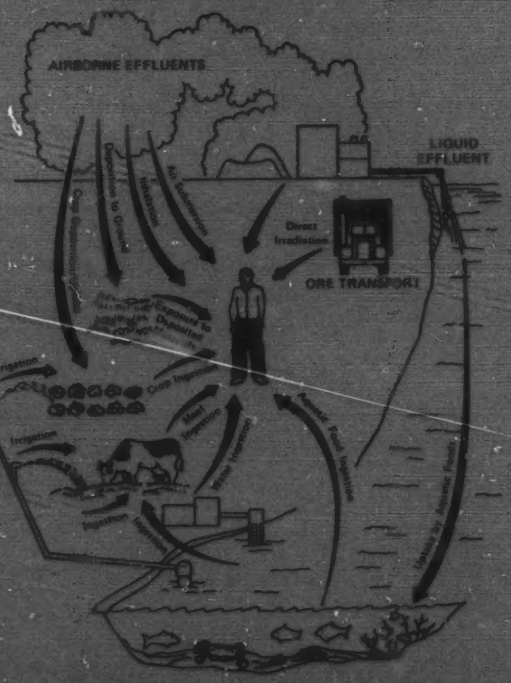

HUMAN-EXPOSURE PATHWAYS FROM
URANIUM-MINING AND -MILLING FACILITIES

NEWARK PUBLIC LIBRARY
JUN 19 1980
U. S. CIVIL PROS.
DEPOSITORY 376

ARGONNE NATIONAL LABORATORY

ARGONNE NATIONAL LABORATORY, ARGONNE, ILLINOIS
Prepared for the U. S. NUCLEAR REGULATORY COMMISSION
under Interagency Agreement DOE 40-550-75

Y 3. N 88:

READEX FICHE

The facilities of Argonne National Laboratory are owned by the United States Government. Under the terms of a contract (W-31-109-Eng-38) among the U. S. Department of Energy, Argonne Universities Association and The University of Chicago, the University employs the staff and operates the Laboratory in accordance with policies and programs formulated, approved and reviewed by the Association.

MEMBERS OF ARGONNE UNIVERSITIES ASSOCIATION

The University of Arizona
Carnegie-Mellon University
Case Western Reserve University
The University of Chicago
University of Cincinnati
Illinois Institute of Technology
University of Illinois
Indiana University
The University of Iowa
Iowa State University
The University of Kansas
Kansas State University
Loyola University of Chicago
Marquette University
The University of Michigan
Michigan State University
University of Minnesota
University of Missouri
Northwestern University
University of Notre Dame
The Ohio State University
Ohio University
The Pennsylvania State University
Purdue University
Saint Louis University
Southern Illinois University
The University of Texas at Austin
Washington University
Wayne State University
The University of Wisconsin-Madison

NOTICE

This report was prepared as an account of work sponsored by an agency of the United States Government. Neither the United States Government nor any agency thereof, or any of their employees, makes any warranty, expressed or implied, or assumes any legal liability or responsibility for any third party's use, or the results of such use, of any information, apparatus, product or process disclosed in this report, or represents that its use by such third party would not infringe privately owned rights.

Available from

GPO Sales Program
Division of Technical Information and Document Control
U. S. Nuclear Regulatory Commission
Washington, D.C. 20555

and

National Technical Information Service
Springfield, Virginia 22161

NUREG/CR-1412
ANL/ES-88

Distribution
Code: RU

ARGONNE NATIONAL LABORATORY
9700 South Cass Avenue
Argonne, Illinois 60439

SYSTEMS FOR CONTINUOUS MEASUREMENT OF AIRBORNE RADON-222 CONCENTRATION AND WORKING LEVEL

by

Michael H. Momeni
Albin J. Zielen
James E. Miranda, Jr.*
Norbert D. Kretz
Walter E. Kisieleski

Division of Environmental Impact Studies

Project Manager
Walter E. Kisieleski

April 1980

Prepared for
Office of Nuclear Regulatory Research
U.S. Nuclear Regulatory Commission
Washington, DC 20555

NRC FIN No. A2209

*Electronics Division

PREFACE

The Argonne National Laboratory, under contract with the U.S. Nuclear Regulatory Commission (USNRC), Division of Safeguards, Fuel Cycle and Environmental Research, has conducted extensive long-term field studies at operating uranium mills to provide input for the Generic Environmental Impact Statement on Uranium Milling being prepared by the USNRC.

The mission of the field study was intended to:

1. Provide measurements that could be used to characterize and estimate rates of release of airborne radioactive effluents (source terms) for uranium-milling activities. This would include release rates of radioactive particulates (specific nuclides) and radon-222 from mill stacks and vents, ore piles, and tailings piles.

2. Provide data that could be used to verify predicted offsite environmental concentrations of radionuclides based on source terms and dispersion calculations.

3. Provide data that could be used to evaluate the potential radiological significance of food-ingestion pathways for airborne effluents released from uranium mills, focusing primarily on ingestion exposures associated with grazing animals and locally raised food crops or garden produce.

4. Serve as a means to test, demonstrate, and evaluate environmental monitoring methods and techniques in order to provide information that could be used in the development of guidance for monitoring programs.

As part of this broad field study, this report describes the design and calibration of a continuous radon and working level monitor as developed by the authors at Argonne National Laboratory. Particular note is given to those factors affecting accuracy and precision. The report further gives an overview of the techniques that have been developed for measuring radon and its daughters in air. Emphasis is on measurements for surveillance and protection in occupational and environmental situations.

The authors express their appreciation to C.J. Roberts, J.M. Peterson, J. Rundo, and H.A. May of Argonne National Laboratory for their reviews of this report. The authors are indebted to the managements and staffs of the Eberline Instrument Corporation, Santa Fe, New Mexico, and the Anaconda Company, Bluewater, New Mexico.

The overall study was conducted by the Division of Environmental Impact Studies of Argonne National Laboratory. This activity was monitored by H.H. Landon (ret.), P.J. Magno (USEPA), and H.J. Miller and L.E. Santos (USNRC).

CONTENTS

	Page
PREFACE	iii
LIST OF FIGURES	vi
LIST OF TABLES	vii
ABSTRACT	1
INTRODUCTION	1
METHODS FOR MEASUREMENT OF RADON CONCENTRATION IN AIR	2
Grab Sampling	3
Scintillation Method	3
Two-Filter Method	3
Integrated Air Sampling	3
Continuous Monitoring	5
Argonne National Laboratory Continuous Radon Monitor	6
Description	6
Calibration Technique	7
Constant Radon Concentration	7
Variable Radon Concentration	10
Calibration Factor	17
Radon Generator	17
VOLTAGE CHARACTERISTICS OF THE CONTINUOUS RADON MONITOR	18
Effect of Voltage Selection and Stability on Counting Rate	20
Calibration Factor	21
Effect of Flow Rate	21
Effect of Humidity	22
RADON DAUGHTERS	24
Measurement of Working Level	24
Theoretical Prediction of Working Level	29
Typical Operation of the CRWM System	37
SUMMARY	38
REFERENCES	40

FIGURES

No.		Page
1	Argonne National Laboratory Continuous Radon Monitor (CRM-100 series)	6
2	Growth and Decay of Radon-222 Daughters	10
3	Relative Alpha-Emitting Radon-Daughter Growth with a Sinusoidally Varying Radon Concentration	16
4	Relative Alpha-Emitting Radon-Daughter Growth with a Sinusoidally Varying Radon Concentration	16
5	Relative Alpha-Emitting Radon-Daughter Growth with a Sinusoidally Varying Radon Concentration	17
6	Radium Bubbler with Bypass	18
7	Radon Count Rate as a Function of High Voltage	19
8	Voltage Characteristic and Dark-Current Noise as Functions of High Voltage	19
9	Calibration Factor as a Function of Flow Rate	22
10	Count Rate as a Function of Radon Concentration	23
11	Continuous Radon and Working-Level Monitor (CRWM-200)	26
12	Continuous Radon and Working-Level Monitor (CRWM-100)	26
13	Photograph of CRWM-200	27
14	Photograph of CRWM-100	27
15	CRWM-200 Enclosure	28
16	CRWM-100 Enclosure	28
17	Working-Level Conversion Factor	37
18	Typical Radon Concentration and Working Level at the Anaconda Uranium Mill, Station 103	38

TABLES

No.		Page
1	Characteristics of Radon-222 and Daughters	7
2	Relative Buildup and Decay of Activity	11
3	Time Integrals of Relative Activities	11
4	Hourly Time-Integrated Activities After Removal of Radon Daughters	15
5	Hourly Time-Integrated Activities After Removal of Radon Daughters	15
6	The Estimated Effect of Voltage Variation as a Function of Radon Concentration and Operating Voltage	20
7	Static Calibration Factor as a Function of Radon Concentration and Count Rate	21
8	Kinetic Calibration Factor as a Function of Humidity	23
9	ANSI Factor as a Function of Time After Collection of the Sample	24
10	Time-Integrated Activities and Working Levels by Hour and by Day	33
11	Time-Integrated Activities and Working Levels by Hour and by Day	34
12	Time-Integrated Activities and Working Levels by Hour and by Day	35
13	Time-Integrated Activities and Working Levels by Hour and by Day	36

SYSTEMS FOR CONTINUOUS MEASUREMENT OF AIRBORNE RADON-222 CONCENTRATION AND WORKING LEVEL

by

M.H. Momeni, A.J. Zielen, J.E. Miranda, Jr.,
N.D. Kretz, and W.E. Kisieleski

Abstract

A system for continuous and simultaneous measurement of airborne radon concentration and working level (WL) has been developed by Argonne National Laboratory. It has detection limits of about 0.05 pCi/L of radon and 5×10^{-4} WL for a one-hour integration period. The system, designated CRWM (Continuous Radon and Working Level Monitor), continuously samples air, flowing at less than 100 L/min, taken about 75 cm above the ground. The air is passed through a 47-mm membrane filter where the airborne particulates and ions are removed. A fraction (1 L/min) of this filtered air is subsequently passed through a 2000-cm^3 aluminum scintillation cell in which radon concentration is determined by counting alpha scintillations. Working level is determined from polonium-218 and polonium-214 activities on the filter using a 490-mm^2 silicon diffused junction detector and a 1024-channel analyzer (alpha spectroscopy). Calibration procedures are discussed. Comparison of calibration factors measured over a relative-humidity range of 0% to 70% did not indicate a moisture dependence. Theoretical bases for measurement of radon and working level are developed. Diurnal variation of radon concentration is simulated using a sinusoidal function. A typical time variation of radon and working level measured in the vicinity of a mill is presented, and measurement techniques are reviewed.

INTRODUCTION

Radon is generated from radium-226, which is present in concentrations from less than 1 pCi/g in soil to several hundred pCi/g in uranium ores. Radon, an inert gas, is readily transported by groundwater and diffuses through soil and some porous rocks. Because of the short half-lives of radon daughters (polonium-218, lead-214, bismuth-214, and polonium-214), a condition near secular radioactive equilibrium is established between radon and its progenies within four hours. Radon concentration in the atmosphere is dependent both on

release rate and dilution in air by dispersion. Also, radon-daughter concentrations are dependent on their rates of ingrowth from the decay of radon and from dilution by dispersion. Inside closed buildings the controlling factor is often the ventilation rate.

Exposure to radon daughters has been associated with lung disorders that include cancer among uranium miners. Radiation dose from exposure to radon alone is significantly less than that from exposure to radon daughters. The radiation dose to the lung from radon daughters in a natural environment is significantly larger than that from other sources of natural radiation.

In many locations, environmental concentrations of radon show significant diurnal variation, sometimes increasing by several times after sunset (Momeni et al. 1979). In addition, radon concentrations depend on regional climate and topography and change significantly within a short time due to varying wind direction and speed. Therefore, the estimation of radon and radon-daughter concentrations presents a unique problem of measurement and sampling.

Several methods for estimation of radon and radon-daughter concentrations have been reported (Budnitz 1974). Up to 1977 the preferred methods for measurement of radon concentration in air had been by either grab sampling or integrated air sampling (Geiger 1967, Shearer and Sill 1969, Costa-Ribeiro et al. 1969, George and Breslin 1977). During the early phases of planning for the Argonne National Laboratory field research at operating mills in 1976, commercial field-grade equipment for measurement of radon concentration was not available. The techniques available did not readily allow measurement of temporal variation of radon concentration in air. The concept behind the design of a continuous radon monitor evolved from previous attempts to measure the fraction of radon-222 exhaled from beagles containing a radium-226 body burden (Momeni et al. 1976). The unpublished method involved an attempt to estimate the radium body burden by the measurement of radon activity in the entrance and exit air passing continuously through an air-tight cage housing a beagle dog contaminated with radium-226. The detector was an aluminum cylinder housing a photomultipler tube and liquid scintillator. Modification of this design to the 1977 prototype system for continuous monitoring of radon concentration in air was made in cooperation with M.R. Morley, H. Beene, and E.L. Geiger of the Eberline Instrument Corporation. In the prototype system the liquid scintillator was replaced by zinc sulfide plated inside a lucite cylinder. Since 1977 the design of the continuous radon monitor has been improved commercially by the Eberline Instrument Corporation, and two other systems have been developed and constructed by Argonne National Laboratory. Since the Budnitz report, continuous-monitoring methods have replaced grab-sampling techniques.

In this report, a summary of available techniques for determining radon concentration and working level is presented. The continuous-monitoring methodology, instrumentation, calibration, theoretical basis for the technique, and simulation of diurnal variation of radon concentration and working level are described.

METHODS FOR MEASUREMENT OF RADON CONCENTRATION IN AIR

Radon concentration in air can be measured in the field using grab sampling, integrated air sampling, and continuous monitoring. However, field

conditions are unlike a research laboratory, with its controlled moisture, temperature, and dust loading. Equipment designed for the field must be rugged and reasonably insensitive to these parameters; an accuracy of ± 20% or better over the entire range of measurement and a sensitivity lower than expected ambient concentrations are often demanded.

GRAB SAMPLING

Scintillation Method

In this method, an evacuated light-tight scintillation cell, a container coated with zinc sulfide, is used for collection of air samples. Alpha radiation emitted from the decay of radon-222, polonium-218, and polonium-214 interacts with the zinc sulfide, producing scintillations that are detected by a photomultiplier tube. The electronic instrumentation includes a high-voltage supply for the photomultiplier tube, preamplifier, amplifer, scaler, timer, and often a printer. Typically, the alpha scintillations are counted four hours after collection of an air sample. The background of these cells is less than three counts per minute (cpm). Their sensitivity for radon-222 is about 6 cpm/(pCi/L), i.e. 0.6 count per alpha particle emitted.

A modification of this system is the application of a conducting surface such as a thin film of gold or silver over the scintillator. On the assumption that the radon daughter polonium-218 is formed as a positive ion, a negative voltage is applied to the conducting surface. Examples of this type of modification are those reported by McLaughlin and Nolan (1969) and Dalu and Dalu (1969). Dalu and Dalu claim a static sensitivity of 0.01 pCi/L for a cell with a volume of 5.25 L.

Two-Filter Method

This method consists basically of a metal cylinder with air filters at both ends (Thomas and LeClare 1970). Air is pumped through the filters for five minutes at a rate of about 10 L/min. The airborne radon daughters and particulates are removed by the upstream filter, and only gases including radon pass through the space between the two filters. A fraction of this radon will decay to polonium-218 during transit, and this daughter is immediately collected downstream on the second filter. After sample collection, this filter is removed and counted for alpha activity. Because of the small amount of activity collected on the second filter, large measurement errors can be expected (Thomas and LeClare 1970).

INTEGRATED AIR SAMPLING

The concentration of radon in air is highly variable and shows strong diurnal variations under calm atmospheric conditions (Momeni et al. 1978, Moses et al. 1963). Average daily radon concentration is dependent on meteorological conditions and may be seasonally dependent. Because of the nonrandom variability of radon concentration in air and lack of knowledge of its temporal dependence, assignment of a confidence limit to data collected by grab sampling is difficult. Thus, integrated air sampling is preferred.

Instruments using this technique are reported by Geiger (1967), Shearer and Sill (1969), Sill and Shearer (1969), George and Breslin (1977), and Costa-Ribeiro et al. (1969).

A simple sampling technique for measurement of average radon concentration is to continuously collect air samples at a constant rate (constant or burst pump) in a plastic bag. A sample of the air collected in the bag is subsequently transferred to evacuated scintillation cells or a Lucas chamber for measurement (Lucas 1957). Sill and Shearer applied this technique using a 40-L mylar bag and collecting air at a rate of 10 mL/min for 48 hours. Correction of the data for decay of radon during collection demands the assumption that the radon concentration in the sampled air is time independent. However, shorter sample-collection times (e.g. 12 h) will not necessitate correction for decay, and a better approximation of the average radon concentration can be made.

An analogous technique is collection of radon in charcoal canisters (Hursh 1954, Moses et al. 1963). Filtered air is passed slowly through charcoal using small pumps. About four hours after collection, the canisters are counted using a gamma spectrometer (NaI), observing either the 352-keV or 609-keV gamma-ray line from lead-214 or bismuth-214, respectively. The efficiency of radon collection on charcoal is dependent on humidity, and the air must be dried before passing it through the canister. The sensitivity of this technique is dependent on the counting-system efficiency but, in general, a radon-222 concentration of 0.1 pCi/L can be measured conveniently. This method, like the previous one, may demand an assumption of time independence of the radon concentration in air to correct for decay during the collection period.

Thermoluminescent dosimeters (lithium fluoride) have been used as detectors in the designs of two types of integrating radon monitors (George and Breslin 1977, George et al. 1976). In one system, which is based on the two-filter method, dosimeter chips are positioned a short distance from the second filter. Alpha and beta emission from radon-daughter buildup on the filter exposes the dosimeters for the duration of contact. In principle, because of the slow fading of high-temperature traps in thermoluminescent dosimeters, an average concentration over a 15-day period can be estimated by this technique. The sensitivity of the system is dependent on the distance of the chips from the filter and on the airflow rate. The dosimeters must be calibrated individually, and duplicate dosimeters should be located within the same collection space to permit correction for background radiation. An adaptation of this system is diffusion of radon through a porous barrier followed by electrostatic collection of polonium-218 ions. Elimination of the pump reduces the fabrication cost of this system significantly. This modified system can readily be operated unattended for long periods. Because of its lower cost, it lends itself to many applications for estimating average environmental radon concentrations. Because a correction for radon decay is not necessary, this system does not require the assumption of constant concentration as do the mylar-bag and charcoal-canister methods. However, due to the inherent variability in response of thermoluminescent dosimeters, even within the same batch, the accuracy of this system may be questioned.

Another technique for measurement of integrated radon concentration was developed by Costa-Ribeiro et al. (1969) using a 28-cm^3 porous-medium chamber

into which radon gas is allowed to diffuse. The detector is a light pipe coated with zinc sulfide and a thin aluminized mylar film. A potential of 60 V between the aluminum conductor and a hemispherical screen causes polonium-218 ions to be electrostatically deposited on the negatively charged aluminum electrode. In an original design, scintillations were recorded on photographic film and radon concentration was determined by use of a calibrated film densitometer. Drawbacks of this system are moisture dependence of the film and the relatively large uncertainty introduced by using a light densitometer.

In general, the passive systems can be used without line electricity and have a low cost per instrument, but they demand high-priced support equipment and labor. They are capable of making long time-average measurements, for reasonable accuracy, and may satisfy the criteria of field-grade equipment if they are designed to withstand extremes of temperature, humidity, and industrial dust.

CONTINUOUS MONITORING

An important attribute of continuous radon monitors, which is lacking in integrating systems, is the ability to measure temporal variations in the radon concentration. From these temporal distributions, average daily radon concentrations and estimates of variability with respect to time can be calculated. One drawback to continuous monitors is a high initial cost of equipment; however, because they operate with little or no attention, the cost of data accumulation over a long time may be comparable to, if not less than, that of techniques requiring more manpower.

Continuous radon monitors have been designed by adapting integral radon-sampling methods, e.g. substitution of a photomultiplier tube and standard radiation counting system (Wrenn 1977) for photographic emulsion and a light densitometer (Costa-Ribeiro et al. 1969).

Pulse-type ionization chambers have been used for measurement of either primary or secondary particles that produce ionization. Such chambers using pulse electronics, or operated as mean-level charge indicators using electrometers, may be used for radon measurement. The earliest reported use of ionization chambers for grab-sampling measurements is by Curtis (1942). The chambers also may be operated as flow-through devices for continuous radon measurement; however, these systems operated under laboratory conditions, and in the presence of moisture fail due to voltage breakdown.

The simplest adaptations of scintillation cells constructed of Erlenmeyer flasks coated inside with zinc sulfide (Van Dilla and Taysum 1955) for continuous measurement was by Harris et al. (1957) who pumped air continuously through the flask. This simple modification has been essentially the principal factor behind many presently operating continuous monitors (Dalu and Dalu 1971, Momeni et al. 1978).

Argonne National Laboratory Continuous Radon Monitor

Description

A prototype continuous radon monitor, fabricated by the Eberline Instrument Corporation for Argonne National Laboratory, has been used in our field studies. Based on experience with the prototype, a system similar to it was later developed at Argonne National Laboratory (CRM-100 series) and is shown in Figure 1. In this system, air containing radon is passed through a dust prefilter and a millipore filter at 1 L/min to remove radon daughters and particulates before circulating through a 2-L aluminum cell (the prototype used a 1.4-L lucite cell). The air passing through the inlet to the cell produces multiple air jets directed toward the wall, increasing air turbulence adjacent to the cell surface and the plateout of airborne ions. The choice of a metallic cell rather than a plastic one is to avoid the diffusion of radon through plastic and slow back diffusion and to avoid the electrostatic behavior of a plastic surface. The metallic cell, either grounded or under a small negative potential, will result in a better charge collection

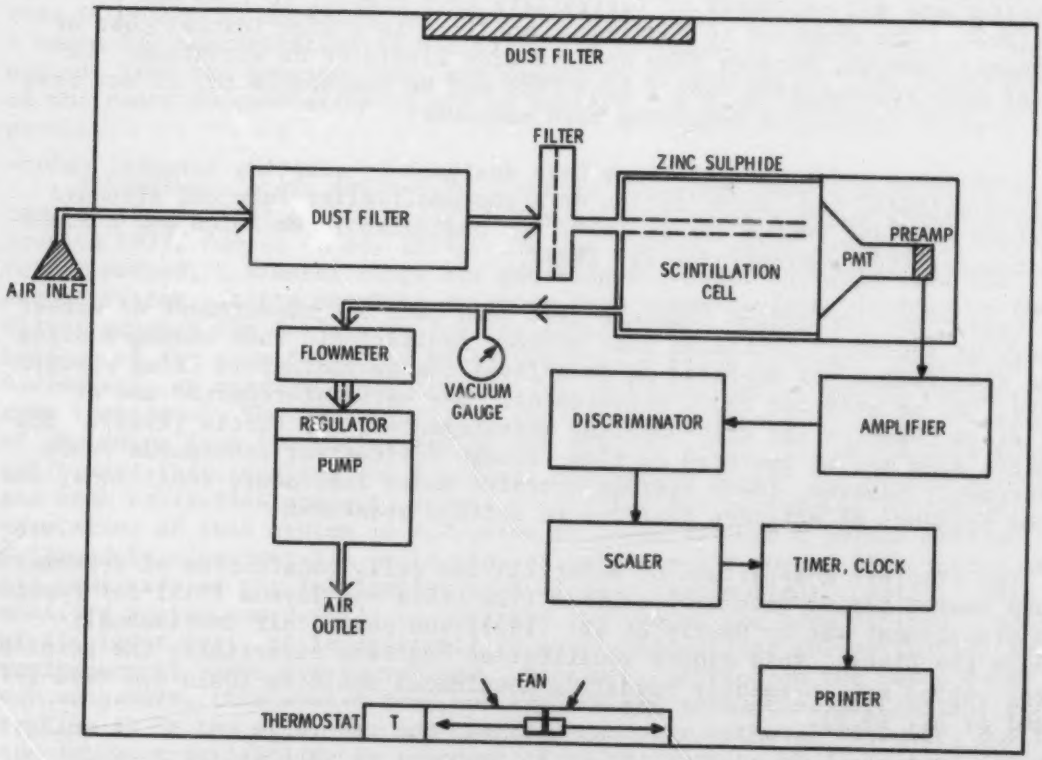

Figure 1. Argonne National Laboratory Continuous Radon Monitor (CRM-100 series).

and plateout of radon-daughter ions. The light-collection efficiency is dependent on the volume and surface area of the cell and on the size of the photomultiplier tube. (A five-cell unit for detection of radon in samples of air obtained at elevations of 1, 8, 16, 24, and 30 m within an open-pit mining area--St. Anthony Mine--using a 1-L aluminum cell was constructed in 1979.)

In routine operation of the continuous monitor, filtered air at a rate of 1 L/min is drawn through the scintillation chamber. During the period of radon transit through the cell, a small fraction of the radon atoms decays to polonium-218 with the emission of 5.49-MeV alpha particles. A fraction of these alphas is detected by the zinc-sulfide scintillator. Before all the polonium-218 ions formed in the decay process are swept from the cell, a portion plates out on the surface of the zinc sulfide, and there decays in succession to lead-214, bismuth-214, and polonium-214. Only the alpha decays of polonium-218 and polonium-214 contribute to the observed count rate. Subsequent decay of lead-210, (the daughter of polonium-214 and a beta emitter with a 22-year half-life) results in a very small contribution to the observed count rate from alphas from polonium-210.

Calibration Technique

Constant Radon Concentration. Let us assume that equal fractions of all the radon daughters generated from the decay of radon in the cell are plated out on the detector wall, and once plated out they are not subsequently removed. Further, let us assume that the amount of radon in the cell is constant (steady-state condition) and is given by the radon activity $A_1 = \chi V$, where χ is the radon concentration in air and V is the cell volume. The total polonium-218 activity in the cell is given by:

$$A'_2(t) = A_1 \left(1 - e^{\lambda_2 t}\right) \qquad (1)$$

where λ_2 is the decay constant of polonium-218 (Table 1). A fraction of polonium-218 (F_1) is deposited on the scintillation surface and is responsible for the observed activity:

Table 1. Characteristics of Radon-222 and Daughters

Radio-Nuclide	*Radio-Nuclide Index*	*Principal Emission*	*Alpha Energy (MeV)*	*Half-Life (minutes)*	*No. of Atoms per pCi*	*Total Potential Alpha Energy (MeV/pCi)*
^{222}Rn	1	α	5.49	5.5 E+03	1.77 E+04	-
^{218}Po	2	α	6.00	3.05 E+00	9.77 E+00	1.34 E+02
^{214}Pb	3	β, α	-	2.68 E+01	8.58 E+01	6.59 E+02
^{214}Bi	4	β, α	-	1.97 E+01	6.31 E+01	4.85 E+02
^{214}Po	5	α	7.68	∿1.0 E-06	8.0 E-06	-
^{210}Pb	6	β	-	∿1.16 E+07	3.7 E+07	-
^{210}Po	7	α	-	∿2.0 E+05	6.3 E+05	-

$$A_2(t) = A_1 F_1 (1 - e^{-\lambda_2 t}) \tag{2}$$

Similarly, if we assume that all the polonium-218 daughters generated on the scintillation surface are not relocated, then for lead-214 the buildup of activity is given by:

$$A_3(t) = A_1 F_1 \left[1 - \left(\frac{\lambda_3}{\lambda_3 - \lambda_2}\right) e^{-\lambda_2 t} - \left(\frac{\lambda_2}{\lambda_2 - \lambda_3}\right) e^{-\lambda_3 t} \right] \tag{3}$$

and for bismuth-214 by:

$$A_4(t) = A_1 F_1 \left[1 - \left(\frac{\lambda_3}{\lambda_3 - \lambda_2}\right)\left(\frac{\lambda_4}{\lambda_4 - \lambda_2}\right) e^{-\lambda_2 t} - \left(\frac{\lambda_2}{\lambda_2 - \lambda_3}\right)\left(\frac{\lambda_4}{\lambda_4 - \lambda_3}\right) e^{-\lambda_3 t} - \left(\frac{\lambda_2}{\lambda_2 - \lambda_4}\right)\left(\frac{\lambda_3}{\lambda_3 - \lambda_4}\right) e^{-\lambda_4 t} \right] \tag{4}$$

(Eq. 2, 3, and 4 are modified forms of the familiar Bateman equations, named for their developer, which describe parent-daughter relations in a more general formulation.) Because the half-life of polonium-214 is very short (about 1 μs), its activity and that of bismuth-214 are in equilibrium: $A_5(t) = A_4(t)$. Eq. 2, 3, and 4 can be reduced to:

$$A_2(t) = A_1 F_1 (1 - e^{-t/4.39}) \tag{5}$$

$$A_3(t) = A_1 F_1 (1 + 0.128\, e^{-t/4.39} - 1.128\, e^{-t/38.6}) \tag{6}$$

and

$$A_4(t) = A_1 F_1 (1 - 0.0235\, e^{-t/4.39} - 4.2594\, e^{-t/38.6} + 3.2829\, e^{-t/28.4}) \tag{7}$$

using the values of λ_2, λ_3, and λ_4 in min^{-1}. During continuous operation with constant radon concentration in air, the daughter activities (I) in the scintillation chamber will increase by buildup. To the extent that the parent activity A_1 remains constant, the daughter activities may be expressed by a buildup factor given by:

$$B(I,t) = \frac{A(I,t)\, F_1}{A_1} \tag{8}$$

where B(I,t) is the buildup of radon daughters under a condition of constant radon concentration. After about four hours of operation, conditions nearly

equal to secular radioactive equilibrium will be established for the radon daughters polonium-218, bismuth-214, and polonium-214. Figure 2 depicts the buildups of radon daughters (solid lines) in the scintillation chamber. Dotted lines show projected activities of radon daughters if air with a constant radon concentration were to flow continuously through the detector. Dot-dash lines represent the decays of residual activities on the detector walls during flushing with radon-free air.

Assuming that flushing of radon from the cell with nitrogen gas will not affect the plated-out radon daughters, then the residual activity within the cell after radon flushing for τ minutes is given by the "Summation Rule" (Evans 1955):

$$D(I,\tau) = B(I,\tau + g) - B(I,\tau) \tag{9}$$

where g is the buildup period and $\tau = t - g$. The cumulative activity for buildup is given by:

$$CB(I,t) = \int_0^t B(I,t)\, dt \tag{10}$$

and for residual activity

$$CD(I,t) = \int_0^t D(I,\tau)\, d\tau \tag{11}$$

Figure 2 and Table 2 depict buildups and decays of radon daughters for g = 60 minutes. Table 3 gives the time integral and total activity (integral sum) of radon daughters for g = 60 minutes and integration period Δt = 60 minutes. Inasmuch as the scintillation chamber is sensitive only to alpha radiation, the observed count for a collection time of Δt is given by:

$$C_1(t) = K\, A_1\, [CB(I=2, \Delta t) + CB(I=5, \Delta t)] + (K\, A_1\, \Delta t) \tag{12}$$

where K is the calibration factor for radon-222, polonium-218, and polonium-214 and includes the F_1 deposition factor. The observed count for time $t \geq g$ is given by:

$$C_2(t) = K\, A_1\, [DB(I=2, \Delta t) + DB(I=5, \Delta t)] \tag{13}$$

Because the operation of radon monitors is continuous, the observed count for an integration period Δt is given by:

$$C(t) = C_1(t) + C_2^1(t) + C_2^2 + C_2^3 + \ldots + C_2^n \tag{14}$$

where C_2^j is for residual activity from radon over a period $t - (j\Delta t)$ (Fig. 2). $C_1(t)$ is from the radon and daughter activity in the cell at time t. The contribution of polonium-218 to C_2^j is small because of its short half-life, but because of the longer half-lives of lead-214 and bismuth-214 their residual activities linger on for several hours (Table 2).

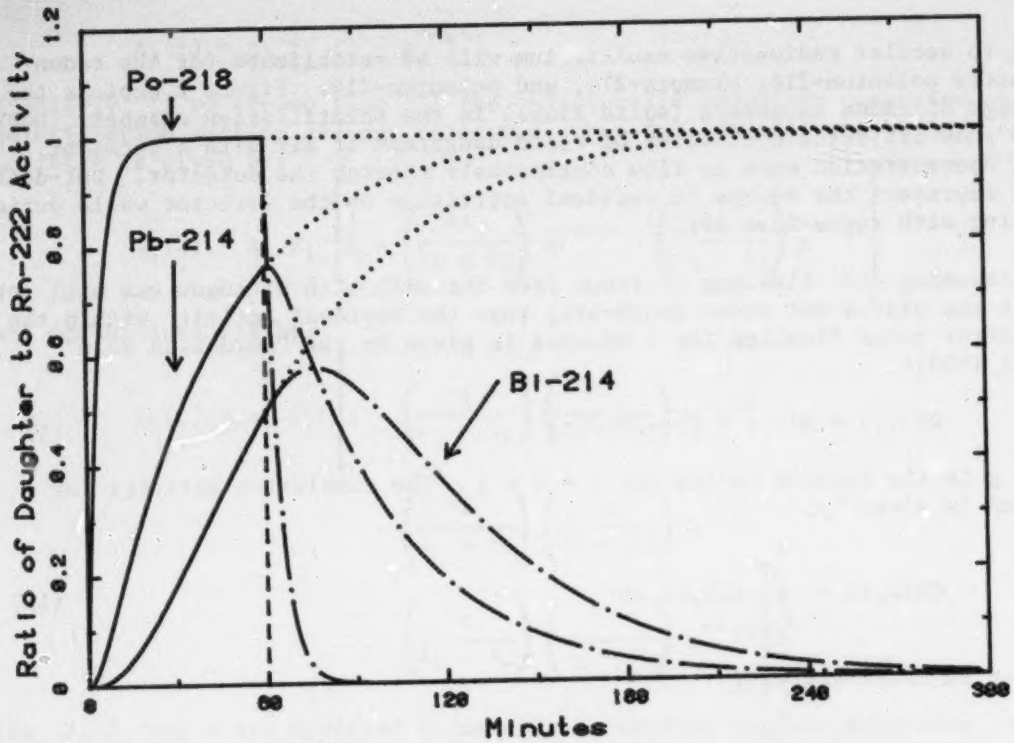

Figure 2. Growth and Decay of Radon-222 Daughters (see text for explanation).

Table 3 gives the alpha activity from buildup of each radon daughter for Δt = 60 minutes, K = 1, and conditions of constant radon concentration. Because of the longer half-lives of lead-214 and bismuth-214 the count contributed by polonium-214 will lag behind the radon pulse. Even though the detection efficiency for radon alphas may not equal those for polonium-218 and polonium-214 alphas, the total alpha count is strongly influenced by radon-222 and polonium-218 alphas (two alphas out of three potential alphas). Thus, the composite peak position should be reasonably representative of the radon-pulse time (Fig. 2).

Variable Radon Concentration. Continuously varying radon concentration is a true-life situation. To model the monitor response under such conditions, we have assumed a sinusoidal radon concentration with a fixed period of 24 hours. But, in general, radon concentration in a given period can be expressed as a sum of harmonic functions with variable periodicities. In this analysis, the mean radon level was assumed to be constant over a period of several days.

Let us assume that the number of atoms of radon-222, N_1, in the scintillation chamber at any time, t, can be expressed as:

Table 2. Relative Buildup and Decay of Activity (ratio of nuclide activity to radon-222 activity)

Total Min.	Decay Min.	Po-218	Pb-214	Bi-214
0.1		0.022522	0.000036	0.000011
0.2		0.044536	0.000129	0.000021
0.5		0.107649	0.000738	0.000056
1.0		0.203709	0.002773	0.000134
2.0		0.365920	0.010119	0.000436
5.0		0.679846	0.050026	0.003516
10.0		0.897501	0.142562	0.018848
15.0		0.967185	0.239411	0.047208
20.0		0.989494	0.329474	0.086091
25.0		0.996636	0.410188	0.132436
30.0		0.998923	0.481607	0.183522
40.0		0.999890	0.599827	0.291606
50.0		0.999989	0.691149	0.398240
60.0	0.0	0.999999	0.761637	0.496872
60.1	0.1	0.977477	0.762218	0.497795
60.2	0.2	0.955463	0.762740	0.498717
60.5	0.5	0.892350	0.763966	0.501473
61.0	1.0	0.796290	0.764960	0.506023
62.0	2.0	0.634079	0.763553	0.514892
65.0	5.0	0.320154	0.740570	0.538632
70.0	10.0	0.102499	0.673476	0.565634
80.0	20.0	0.010506	0.528550	0.574084
100.0	40.0	0.000110	0.315607	0.486131
120.0	60.0	0.000001	0.187994	0.360925
150.0	90.0	0.000000	0.086419	0.204983
180.0	120.0	0.000000	0.039726	0.107815
210.0	150.0	0.000000	0.018262	0.054285
240.0	180.0	0.000000	0.008395	0.026597
300.0	240.0	0.000000	0.001774	0.006082
360.0	300.0	0.000000	0.000375	0.001341
420.0	360.0	0.000000	0.000079	0.000290
480.0	420.0	0.000000	0.000017	0.000062
540.0	480.0	0.000000	0.000004	0.000013
600.0	540.0	0.000000	0.000001	0.000003
660.0	600.0	0.000000	0.000000	0.000001

Table 3. Time Integrals of Relative Activities

INTERVAL (MIN.)	Po-218 INTEGRAL	Po-218 INT. SUM	Pb-214 INTEGRAL	Pb-214 INT. SUM	Bi-214 INTEGRAL	Bi-214 INT. SUM
0.0- 60.0	55.61001	55.610	26.22195	26.222	12.35024	12.350
60.0-120.0	4.38999	4.390	26.52149	26.521	30.32104	30.321
120.0-180.0	0.00001	4.390	5.72314	32.245	12.89898	43.220
180.0-240.0	0.00000	4.390	1.20939	33.454	3.51332	46.733
240.0-300.0	0.00000	4.390	0.25556	33.710	0.83765	47.571
300.0-360.0	0.00000	4.390	0.05400	33.764	0.18852	47.760
360.0-420.0	0.00000	4.390	0.01141	33.775	0.04123	47.801
420.0-480.0	0.00000	4.390	0.00241	33.777	0.00888	47.810
480.0-540.0	0.00000	4.390	0.00051	33.778	0.00190	47.812
540.0-600.0	0.00000	4.390	0.00011	33.778	0.00040	47.812
600.0-660.0	0.00000	4.390	0.00002	33.778	0.00009	47.812

$$N_1 = N_1^0 \ (1 + a \sin kt) \tag{15}$$

where N_1^0 = mean number of radon-222 atoms in the chamber,
a = relative amplitude of sine wave, range 0 to 1,
$k = 2\pi/60p$,
p = sine period in hours, and
t = time in minutes.

Because all the radon-222 daughters in air are filtered out before the radon sample enters the scintillation chamber, the differential equation for the j-th atoms, N_j, with the restraints $j > 1$ and $N = 0$ at $t = 0$ is written as:

$$dN_j/dt = \lambda_{j-1} N_{j-1} - \lambda_j N_j \tag{16}$$

The solutions of Eq. 16 for j = 2 to 4 are:

$$N_2 = \lambda_1 N_1^0 \left\{(1 - e^{-\lambda_2 t})/\lambda_2 + \frac{a}{\lambda_2^2 + k^2} (k e^{-\lambda_2 t} + \lambda_2 \sin kt - k \cos kt)\right\} \tag{17}$$

and

$$N_3 = \lambda_1 \lambda_2 N_1^0 \left\{1/(\lambda_2 \lambda_3) + I_3 e^{-\lambda_3 t} + \frac{a}{(\lambda_2^2 + k^2)(\lambda_3^2 + k^2)} [(\lambda_2 \lambda_3 - k^2) \sin kt - k (\lambda_2 + \lambda_3) \cos kt] + \frac{e^{-\lambda_2 t}}{\lambda_3 - \lambda_2} \left(\frac{a k}{\lambda_2^2 + k^2} - \frac{1}{\lambda^2}\right)\right\} \tag{18}$$

where

$$I_3 = -\frac{1}{\lambda_2 \lambda_3} + \frac{1}{\lambda_2^2 + k^2} \left[\frac{a k (\lambda_2 + \lambda_3)}{\lambda_3^2 + k^2} + \frac{\lambda_2^2 + k^2 - a k \lambda_2}{(\lambda_3 - \lambda_2) \lambda_2}\right] \tag{19}$$

and

$$N_4 = \lambda_1 \lambda_2 \lambda_3 N_1^0 \left\{1/(\lambda_2 \lambda_3 \lambda_4) + I_4 e^{-\lambda_4 t} + \frac{I_3 e^{-\lambda_3 t}}{\lambda_4 - \lambda_3} + \frac{e^{-\lambda_2 t}}{(\lambda_4 - \lambda_3)(\lambda_3 - \lambda_2)} \left(\frac{a k}{\lambda_2^2 + k^2} - \frac{1}{\lambda_2}\right) + \frac{a}{(\lambda_2^2 + k^2)(\lambda_3^2 + k^2)(\lambda_4^2 + k^2)} \left[\lambda_2 \lambda_3 \lambda_4 - k^2 (\lambda_2 + \lambda_3 + \lambda_4) \sin kt - k (\lambda_2 \lambda_3 + \lambda_2 \lambda_4 + \lambda_3 \lambda_4 - k^2) \cos kt\right]\right\} \tag{20}$$

where $$I_4 = \frac{I_3}{\lambda_4 - \lambda_3} - \frac{1}{\lambda_2 \lambda_3 \lambda_4}$$

$$- \frac{1}{(\lambda_4 - \lambda_2)(\lambda_3 - \lambda_2)} \left(\frac{a\,k}{\lambda_2^2 + k^2} - \frac{1}{\lambda_2} \right)$$

$$+ \frac{a\,k\,(\lambda_2 \lambda_3 + \lambda_2 \lambda_4 + \lambda_3 \lambda_4 - k^2)}{(\lambda_2^2 + k^2)(\lambda_3^2 + k^2)(\lambda_4^2 + k^2)} \tag{21}$$

For monitoring periods greater than four hours, the exponential terms in Eq. 17, 18, and 20 become negligible. The equations can then be simplified to:

$$N_2 = \lambda_1 N_1^0 \left\{ \frac{1}{\lambda_2} + \frac{a}{\lambda_2^2 + k^2} (\lambda_2 \sin kt - k \cos kt) \right\} \tag{22}$$

$$N_3 = \lambda_1 N_1^0 \left\{ \frac{1}{\lambda_3} + \frac{a\,\lambda_2}{(\lambda_2^2 + k^2)(\lambda_3^2 + k^2)} \left[(\lambda_2 \lambda_3 - k^2) \sin kt - k(\lambda_2 + \lambda_3) \cos kt \right] \right\} \tag{23}$$

and $$N_4 = \lambda_1 N_1^0 \left\{ \frac{1}{\lambda_4} + \frac{a\,\lambda_2 \lambda_3}{(\lambda_2^2 + k^2)(\lambda_3^2 + k^2)(\lambda_4^2 + k^2)} \left[\lambda_2 \lambda_3 \lambda_4 - k^2 (\lambda_2 + \lambda_3 + \lambda_4) \sin kt - k(\lambda_2 \lambda_3 + \lambda_2 \lambda_4 + \lambda_3 \lambda_4 - k^2) \cos kt \right] \right\} \tag{24}$$

The time integrated activities, A_j, are obtained as follows:

$$A_j = \int_{t_1}^{t_2} \lambda_j N_j \, dt \tag{25}$$

$$A_1 = \lambda_1 N_1^0 \, [t_2 - t_1 - a\, f_c/k] \tag{26}$$

$$A_2 = \lambda_1 N_1^0 \left[t_2 - t_1 - \frac{a\,\lambda_2}{\lambda_2^2 + k^2} \left(\frac{\lambda_2 f_c}{k} + f_s \right) \right] \tag{27}$$

and $$A_4 = \lambda_1 N_1^0 \, [t_2 - t_1 - Q_1 (Q_2 f_c/k + Q_3 f_s)] \tag{28}$$

where $$f_c = \cos kt_2 - \cos kt_1 \tag{29}$$

$$f_s = \sin kt_2 - \sin kt_1 \tag{30}$$

$$Q_1 = \frac{a\ \lambda_2\ \lambda_3\ \lambda_4}{(\lambda_2{}^2 + k^2)\ (\lambda_3{}^2 + k^2)\ (\lambda_4{}^2 + k^2)} \tag{31}$$

$$Q_2 = \lambda_2\ \lambda_3\ \lambda_4 - k^2\ (\lambda_2 + \lambda_3 + \lambda_4) \tag{32}$$

and

$$Q_3 = \lambda_2\ \lambda_3 + \lambda_2\ \lambda_4 + \lambda_3\ \lambda_4 - k^2 \tag{33}$$

Because only alphas are detected, and with $A_4 = A_5$, the observed count for a collection time $\Delta t = t_2 - t_1$ is:

$$C = K\ (A_1 + A_2 + A_4) \tag{34}$$

$$C = K\ \lambda_1\ N_1{}^0 \left[3\ \Delta t - \frac{a\ f_c}{k} - \frac{a\ \lambda_2}{\lambda_2{}^2 + k^2} \left(\frac{\lambda_2\ f_c}{k} + f_s\right) - Q_1 \left(\frac{Q_2\ f_c}{k} + Q_3\ f_s\right)\right] \tag{35}$$

Tables 4 and 5 present calculations of hourly counts of the monitor, assuming that $K\ \lambda_1\ N_1{}^0 = 1$, with relative sinusoidal amplitudes of 0.5 and 1.0, respectively. Figure 3 shows growth of alpha activity over a six-hour period from sinusoidal radon activity with a relative amplitude of 0.5. Polonium-218 activity parallels the radon activity within the first 20 minutes, but bismuth-214 activity lags behind that of radon for several hours. Growth of alpha activity over a 24-hour period from sinusoidal radon activity with a relative amplitude of 1.0 is shown in Figure 4. Except for the first few minutes, the activities of polonium-218 and bismuth-214 are equal, but the latter lags behind the radon activity. (Due to the 1-μs polonium-214 half-life, its activity and that of bismuth-214 are in equilibrium.) The error given in the tables, i.e. the difference between actual and predicted radon activities, is obtained by subtracting the value in the radon-222 column from that in the column headed Total/3. The factor three arises from the detection of three alphas for the decay of each radon atom. Total/3 is the mean of the radon-222, polonium-218, and polonium-214 activities, assuming that detection efficiency for radon alphas is equal to that for the other alphas. The results show that the error in hourly readings is about proportional to the cycle amplitude. However, even in the worst case where the radon level drops to zero, the maximum hourly error is only about 10% of the mean radon activity. But the error in the daily (or, more properly, "cycle-period") average is zero, and the simulation represents the actual input data (Fig. 5). Except for the first few hours after starting the system, the variations in daughter activities are synchronous with that of radon activity.

The diurnal changes in radon concentration vary in amplitude, and are assumed to rise to and fall from the peaks symmetrically. The time of maximum radon concentration may be dependent on topography and the season. Amplitude changes may also be caused by frontal air-mass movements that break up local thermal inversions.

Table 4. Hourly Time-Integrated Activities (pCi/L) After Removal of Radon Daughters (sine period = 24 h, relative amplitude = 0.5)

Hour	Rn-222	Po-218	Po-214	Total/3	Error
1	1.065077	1.055566	0.913241	1.01129	-0.05378
2	1.190796	1.181885	1.040436	1.13771	-0.05309
3	1.303512	1.295809	1.164876	1.25473	-0.04878
4	1.395545	1.389574	1.278079	1.35440	-0.04115
5	1.460622	1.456790	1.372332	1.42991	-0.03071
6	1.494308	1.492877	1.441211	1.47613	-0.01818
7	1.494308	1.495375	1.480022	1.48990	-0.00441
8	1.460622	1.464114	1.486120	1.47029	0.00966
9	1.395545	1.401224	1.459090	1.41862	0.02308
10	1.303512	1.310992	1.400774	1.33843	0.03491
11	1.190796	1.199566	1.315146	1.23517	0.04437
12	1.065077	1.074540	1.208041	1.11589	0.05081
13	0.934923	0.944434	1.086759	0.98871	0.05378
14	0.809204	0.818115	0.959564	0.86229	0.05309
15	0.696488	0.704191	0.835124	0.74527	0.04878
16	0.604455	0.610426	0.721921	0.64560	0.04115
17	0.539378	0.543210	0.627668	0.57009	0.03071
18	0.505692	0.507123	0.558789	0.52387	0.01818
19	0.505692	0.504625	0.519978	0.51010	0.00441
20	0.539378	0.535886	0.513080	0.52971	-0.00966
21	0.604455	0.598776	0.540910	0.58138	-0.02308
22	0.696488	0.689008	0.599226	0.66157	-0.03491
23	0.809204	0.800434	0.684854	0.76483	-0.04437
24	0.934923	0.925460	0.791959	0.88411	-0.05081
Sums:	24.000000	24.000000	24.000000	24.00000	0.00000

Table 5. Hourly Time-Integrated Activities (pCi/L) After Removal of Radon Daughters (sine period = 24 h, relative amplitude = 1.0)

Hour	Rn-222	Po-218	Po-214	Total/3	Error
1	1.130154	1.111132	0.826482	1.02259	-0.10756
2	1.381592	1.363770	1.080873	1.27541	-0.10618
3	1.607024	1.591618	1.329751	1.50946	-0.09756
4	1.791090	1.779148	1.556158	1.70880	-0.08229
5	1.921243	1.913580	1.744663	1.85983	-0.06141
6	1.988616	1.985754	1.882421	1.95226	-0.03635
7	1.988616	1.990750	1.960044	1.97980	-0.00881
8	1.921243	1.928228	1.972241	1.94057	0.01933
9	1.791090	1.802448	1.918181	1.83724	0.04615
10	1.607024	1.621984	1.801549	1.67685	0.06983
11	1.381592	1.399132	1.630292	1.47034	0.08875
12	1.130154	1.149080	1.416083	1.23177	0.10162
13	0.869846	0.888868	1.173518	0.97741	0.10756
14	0.618408	0.636230	0.919127	0.72459	0.10618
15	0.392976	0.408382	0.670249	0.49054	0.09756
16	0.208910	0.220852	0.443842	0.29120	0.08229
17	0.078757	-0.086420	0.255337	0.14017	0.06141
18	0.011384	0.014246	0.117579	0.04774	0.03635
19	0.011384	0.009250	0.039956	0.02020	0.00881
20	0.078757	0.071772	0.027759	0.05943	-0.01933
21	0.208910	0.197552	0.081819	0.16276	-0.04615
22	0.392976	0.378016	0.198451	0.32315	-0.06983
23	0.618408	0.600868	0.369708	0.52966	-0.08875
24	0.869846	0.850920	0.583917	0.76823	-0.10162
Sums:	24.000000	24.000000	24.000000	24.00000	0.00000

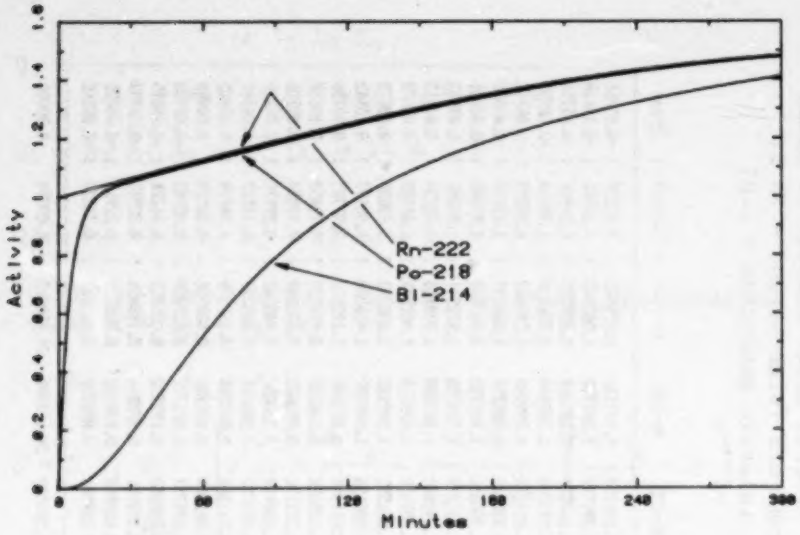

Figure 3. Relative Alpha-Emitting Radon-Daughter Growth with a Sinusoidally Varying Radon Concentration (sine period = 24 h, relative amplitude = 0.5).

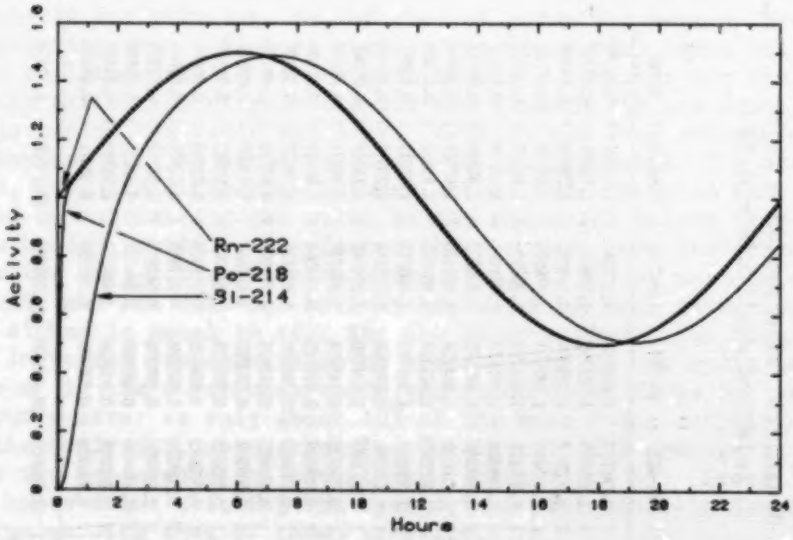

Figure 4. Relative Alpha-Emitting Radon-Daughter Growth with a Sinusoidally Varying Radon Concentration (sine period = 24 h, relative amplitude = 1.0).

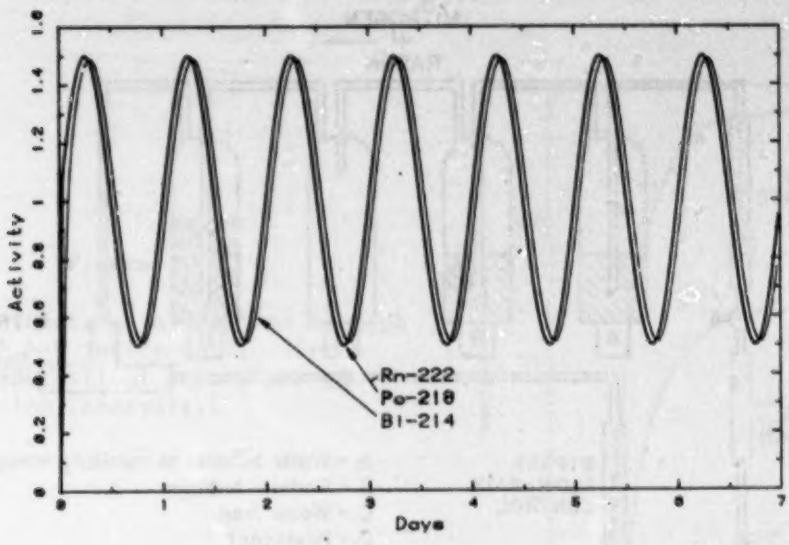

Figure 5. Relative Alpha-Emitting Radon-Daughter Growth with a Sinusoidally Varying Radon Concentration (sine period = 24 h, relative amplitude = 0.5).

Calibration Factor. The calibration factor K is dependent on the plateout of daughters on the scintillation surface and relocation of the attached fraction from the surface. These phenomena are functions of air-flow rate, chamber design, and possibly humidity.

A continuous radon monitor calibrated at sea level (K_0) under standard conditions of temperature and pressure (P_0, T_0), but used under different conditions (P,T) has a calibration factor:

$$K = \left(\frac{P\ T_0}{P_0\ T}\right) K_0 \tag{36}$$

Operation of the monitor between the temperatures of 240 K and 315 K and pressures of about 90 and 100 kPa produces a calibration-factor variation of about 7%.

Radon Generator

Radon was generated from a radium-226 standard in a "radium bubbler" (Fig. 6). The rate of flow of nitrogen through the bubbler was maintained at less than 1 mL/min, but was recombined with a larger nitrogen flow rate after radon generation.

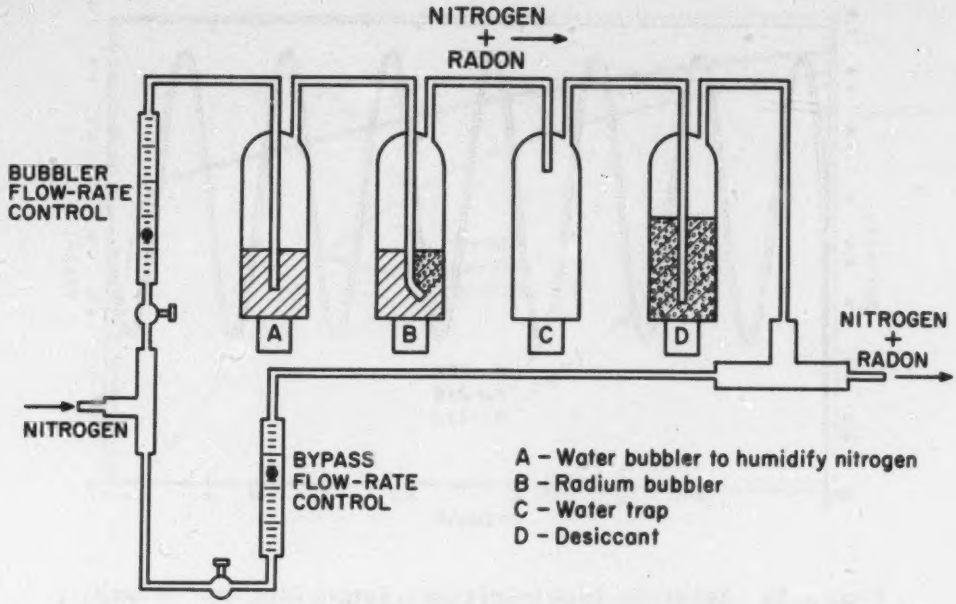

Figure 6. Radium Bubbler with Bypass.

Inasmuch as the radon generator contains radium-226 in solution, it is not readily portable for operation in the field. Radon generators constructed with solid matrices provide a convenient system for calibration of the monitors under field conditions. Our preliminary results suggest that the rate of radon generation may be flow-rate dependent for some matrices operated at rates greater than 5 L/min, but to be independent of flow rate from 0.5 to 5 L/min.

VOLTAGE CHARACTERISTICS OF THE CONTINUOUS RADON MONITOR

The continuous radon monitor (CRM-100) was calibrated using the radon generator depicted in Figure 6. The count rate obtained from the radon monitor (Fig. 1), containing a known radon activity within the cell under secular radioactive equilibrium, was observed as a function of phototube voltage. The voltage to the phototube was gradually increased until occasional counts were observed, then the voltage was increased stepwise. This procedure was repeated for three different radon concentrations. The cell was then cleared of radon, and background and dark-current noise were measured after decay of radon-daughter residual activities. Voltage-characteristic curves are presented in Figures 7 and 8.

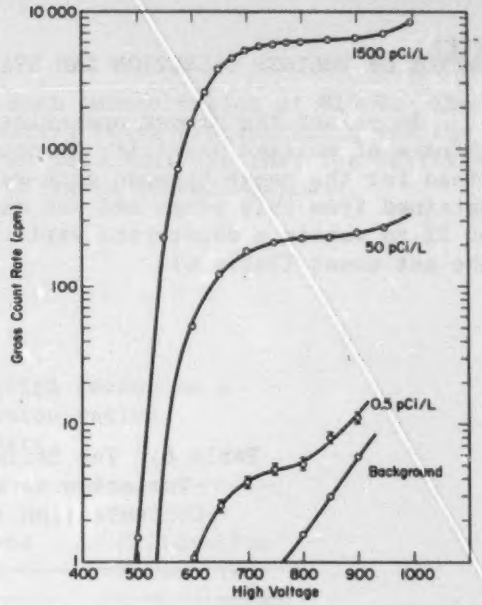

Figure 7.

Radon Count Rate as a Function of High Voltage, 1.4-L Lucite Cell. (Error bars are statistical errors for one-hour counting intervals.)

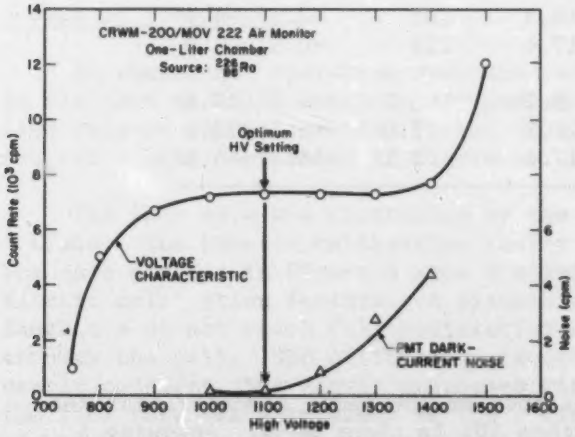

Figure 8.

Voltage Characteristic and Dark-Current Noise as Functions of High Voltage, Aluminum Cell.

The voltage characteristics described by these curves vary with radon concentration in the cell. The selection of an operating voltage on the basis of the higher-concentration curves seems to lead to errors at lower concentrations.

EFFECT OF VOLTAGE SELECTION AND STABILITY ON COUNTING RATE

To select the proper operating voltage it is necessary to quantify the effects of voltage stability on counting rate. The slope (cpm/V) was determined for the range between each voltage step. Variation in count rate was obtained from this slope and was multiplied by the actual voltage variation of 2% to obtain a count-rate variation. Subsequently, this was divided by the net count (Table 6).

Table 6. The Estimated Effect of Voltage Variation as a Function of Radon Concentration and Operating Voltage

Radon Concentration (pCi/L)	*Operating Voltage (V)*	*± 2% Variation (±V)*	*Net Count Rate (cpm)*	*Count Rate Variation (%)*	
1200	760	15.2	5230	+3.0	-7.1
	815	16.3	5800	+1.7	-2.7
	870	17.4	6150	+1.0	-1.6
50	760	15.2	174	+4.8	-8.0
	815	16.3	205	+2.0	-4.1
	870	17.4	219	+0.5	-1.9
0.5	760	15.2	1.7	+14.3	-18.4
	815	16.3	2.0	+5.1	-12.1
	870	17.4	2.1	+46.4	-4.8

It is evident from this analysis that at low radon concentration the plateau length for an error of less than 10% is about 60 V. Assuming a voltage stability of ± 15 V, the selection of operating voltage is restricted to a mid-plateau voltage ± 15 V.

CALIBRATION FACTOR

The static calibration factor at zero flow rate (K_s) is defined as the net count rate in cpm obtained for each pCi/L contained in the monitor cell:

$$K_s = \frac{cpm}{pCi/L} \tag{37}$$

K_s was determined using the data for each concentration at 815 V. The data in Table 7 include the error in estimating radon concentration and the statistical error of the measurement. These data indicate that the calibration factor is constant over a wide range of radon concentrations.

Table 7. Static Calibration Factor as a Function of Radon Concentration and Count Rate

Radon Concentration in Cell (pCi/L)		*Net Count Rate (cpm)*		*Calibration Factor (K_s)*	
1200	±24	5800	±76	4.83	±0.115
45	±1	205	±4.5	4.56	±0.141
0.45	±0.1	2.0	±0.3	4.44	±1.19

Effect of Flow Rate

In the normal operating mode the radon monitor measures radon activity in air that is being continuously pumped through the cell. The effect of flow rate on the calibration factor (dynamic calibration) was obtained using the radon generator shown in Figure 6.

The flow rate was controlled by the bypass line and was varied from 0 to 5 L/min. The kinetic calibration factor was determined for various rates. The data plotted in Figure 9 show a significant difference between static and kinetic calibration factors. A plausible explanation may be that the radon daughters do not reach full equilibrium and are washed out by the gas moving through the cell. The calibration factor corresponding to 0.5 to 2 L/min is nearly constant, but slowly decreases with increasing flow rate. Therefore, the flow rate was maintained at 1.0 ± 0.2 L/min, a rate at which small variations should not affect the calibration factor.

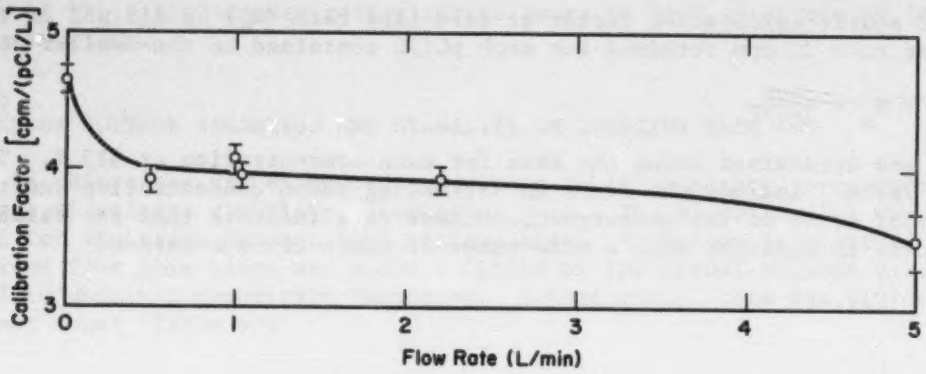

Figure 9. Calibration Factor as a Function of Flow Rate.

Based on a typical measured background for the scintillation cells and phototube dark-current noise, the observed count rate and error (two standard deviations) for various concentrations of radon in air are given in Figure 10. The lowest detectable concentration was estimated from the count rate corresponding to the background count rate plus twice its standard deviation. The lowest level based on this stringent criterion of analysis for one hour of counting is 0.15 pCi/L for Unit No. 2 of CRM-100. This value is directly dependent on the background of the cell, which varies from 30 to 240 counts per hour for uncontaminated cells. The cell background and counting interval directly affect the detection limit. Under laboratory conditions, activities as low as 0.05 pCi/L may be detected. The experimental uncertainity in calibration may indicate an overall precision of about ± 10%, not including counting error. But under two standard deviations, the counting error of the mean value of 0.05 pCi/L is larger than 10%. However, in practice the gross-minus-background count plus two standard deviations may be effectively undetectable.

Effect of Humidity

During field measurements, the radon monitor is subjected to a wide range of relative humidities. To determine the effect of moisture on the cell calibration factor, a second bypass was added to the radon generator. This line was connected to a gas-washing bottle containing glass beads and water. After mixing with the radon from the bubbler, the resulting humidified nitrogen gas was passed through the cell. Measurement of the calibration factor over a relative-humidity range of 0% to 70% indicates that it is independent of moisture, as shown in Table 8.

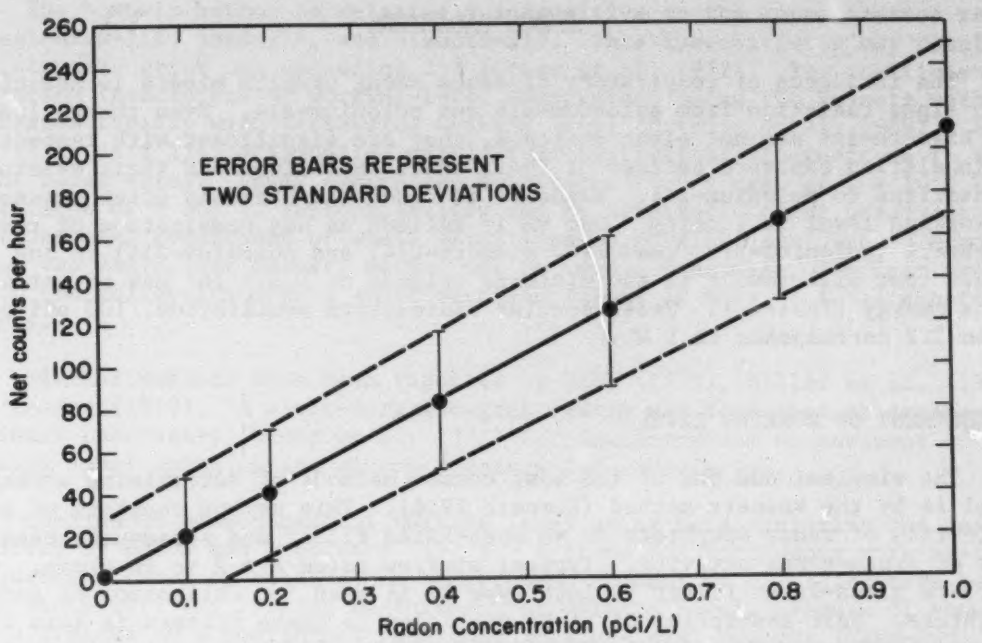

Figure 10. Count Rate as a Function of Radon Concentration (Unit No. 2 of CRM-100).

Table 8. Kinetic Calibration Factor as a Function of Humidity

Relative Humidity (%)	*Calibration Factor (K_s)*
0	4.19 ±1.5
70	4.18 ±1.5
90	3.92 ±1.5

RADON DAUGHTERS

The incidence of respiratory diseases among uranium miners is associated with alpha radiation from polonium-218 and polonium-214. Even though lead-214 and bismuth-214 are not alpha emitters, they are significant with respect to inhalation exposure because of their short half-lives and their eventual transitions to polonium-214. Exposure to radon daughters is often expressed in working level (WL) units. One WL is defined as any combination of radon daughters (polonium-218, lead-214, bismuth-214, and polonium-214) in one liter of air that will result in the ultimate release of 1.3×10^5 MeV of potential alpha energy (Table 1). Under secular radioactive equilibrium, 100 pCi of radon-222 corresponds to 1 WL.

MEASUREMENT OF WORKING LEVEL

The simplest and one of the most common methods of determining working level is by the Kusnetz method (Kusnetz 1956). This method consists of grab collection of radon daughters on an open-faced filter and subsequent measurement of gross-alpha activity. Typical airflow rates are 2 to 10 L/min. Often a 2.5-cm glass-fiber filter (Gelman type E) is used for collection of radon daughters. Self absorption of alpha particles in these filters is less than 10% and they are rugged for field use. Typical collection periods last five minutes. Alpha counting is initiated from 40 to 90 minutes after the sampling. Factors for determination of working level from these parameters are given in American National Standards Institute (ANSI) N13-8-1973. Working level is computed by:

$$WL = cpm/(E\ V\ F) \tag{38}$$

where cpm is the measured alpha count rate, E is the detector efficiency, V is the volume (in liters) of air passed through the filter, and F is the ANSI factor. Values of F are tabulated in Table 9.

Table 9. ANSI Factor as a Function of Time After Collection of the Sample

Time (minutes)	*ANSI Factor (F)*
40	150
45	140
50	130
55	120
60	110
70	90
90	60

The Kusnetz method is relatively insensitive to the concentration ratios of polonium-218, lead-214, and bismuth-214. This insensitivity may result in an intrinsic error not exceeding 25% (Groer et al. 1972). The coefficient of variation (precision) of working-level measurement using the Kusnetz method increases rapidly with decreasing working level (Breslin et al. 1969). At 0.3 WL it is ± 15%, originating mainly from statistical fluctuations in the alpha count rates. Under controlled conditions with a mean of 1×10^{-4} WL, variations of ± 30% in reproducibility can be detected. Under steady-state environmental conditions or where variations in working level from a mean value are small, the Kusnetz method can be used. Otherwise, its main drawback is in the collection over a short duration (about 10 min) of a representative sample.

Similar methods have been reported by Hill (1975), Miller et al. (1976), and Thomas (1972). A short-duration-grab system was developed at Argonne National Laboratory (Groer et al. 1972) for instantaneous measurement of working level using online microprocessors for computation.

Continuous measurement of working level using beta radiation has been reported by Holub and Droullard (1977). Systems for continuous working-level measurement based on total-alpha measurement (Momeni et al. 1978) have been used since 1977 for routine measurement of working level. Figure 11 shows a block diagram of a continuous radon and working-level monitor (CRWM-200). A simpler version (CRWM-100) was developed in cooperation with M.R. Morley, H. Beene, and E.L. Geiger of the Eberline Instrument Corporation and was constructed by that company (Fig. 12). Figures 13 and 14 show photographs of these systems. CRWM-200 uses a mass-regulated pump, whereas the earlier version (CRWM-100) is volume regulated. The radon cell in CRWM-200 is constructed of aluminum with a volume of either 1 L or 2 L, whereas in CRWM-100 it is lucite (closed end) with a volume of 1.4 L. CRWM-200 uses a 1024-channel analyzer (alpha spectroscopy), whereas CRWM-100 collects total-alpha counts. Both systems are enclosed in weatherproof containers (Figs. 15 and 16). The air inlets are about 75 cm from the ground. The temperature inside each system is regulated to reduce condensation within the cell. The filter holder in the CRWM-200 series was extensively modified to minimize air leakage around the filter. The CRWM-200 is capable of 100-L/min flow rates, but both systems are operated at 10 L/min and 25 L/min for CRWM-100 and CRWM-200, respectively.

Operation of both systems is similar. Air at a constant flow rate is passed through a 47-mm membrane filter where the airborne particulates and ions are removed. A fraction (1 L/min) of the radon-free air is subsequently passed through the radon scintillation cell. Both systems incorporate inline filters to reduce contamination of the radon chamber from accidental leakage due to a failing primary filter.

Both systems use silicon diffused junction detectors (490 mm^2) for measurement of alpha particles. The detector background is less than five counts per hour under the polonium-218 and polonium-214 peaks. During one year of continuous operation under field conditions these detectors have not shown any serious degradation in efficiency or background. Overall, the efficiency of the detectors using thin alpha sources is between 10% and 15%. The detection limit of these systems is about 5×10^{-4} WL. After correction

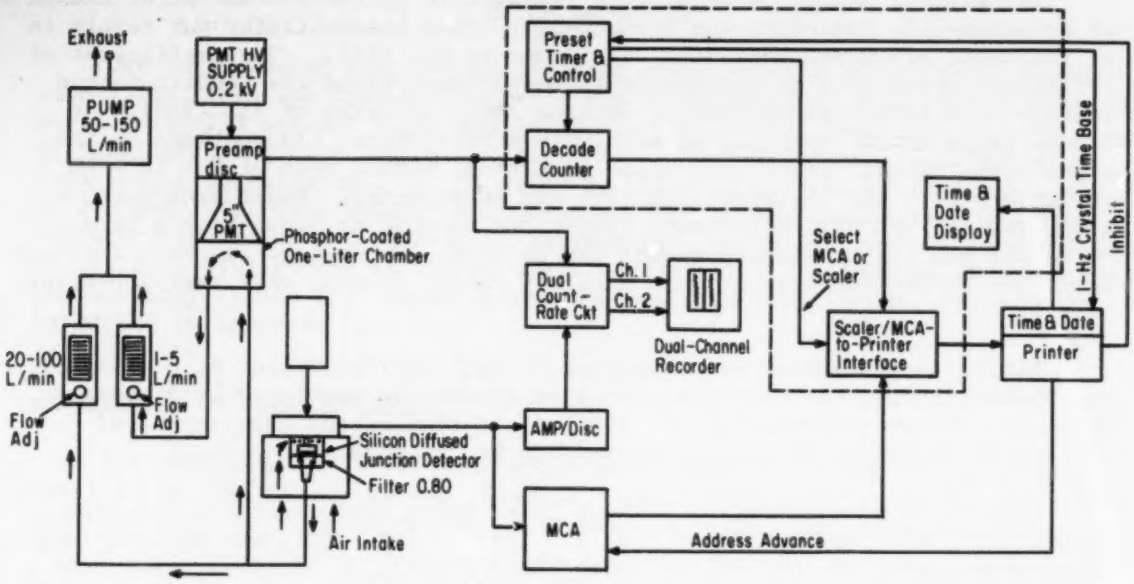

Figure 11. Continuous Radon and Working-Level Monitor (CRWM-200/MOV 222).

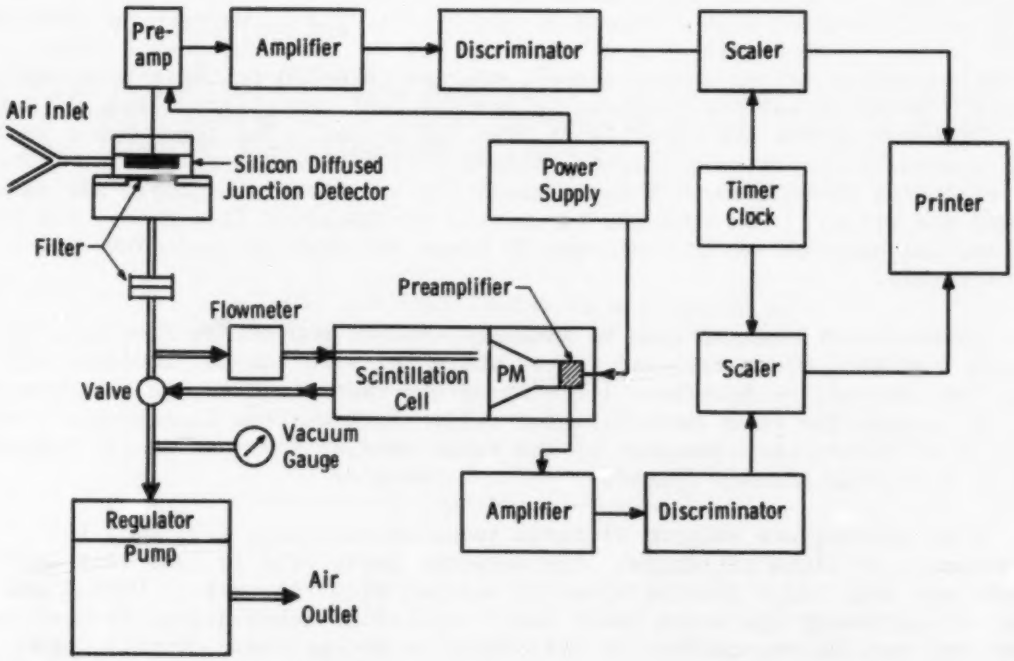

Figure 12. Continuous Radon and Working-Level Monitor (CRWM-100 series).

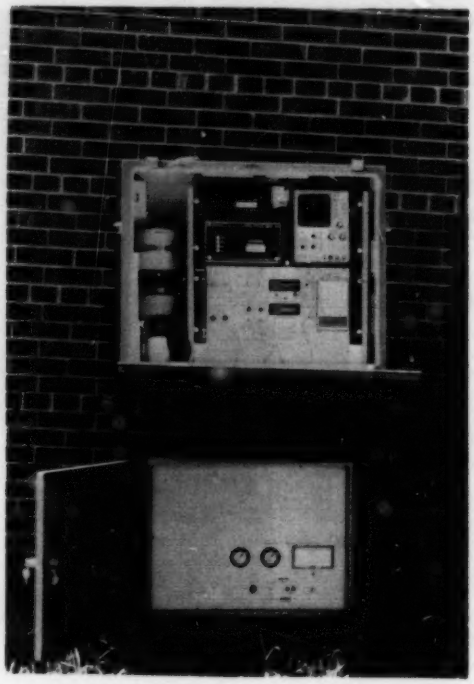

Figure 13.

Photograph of CRWM-200.

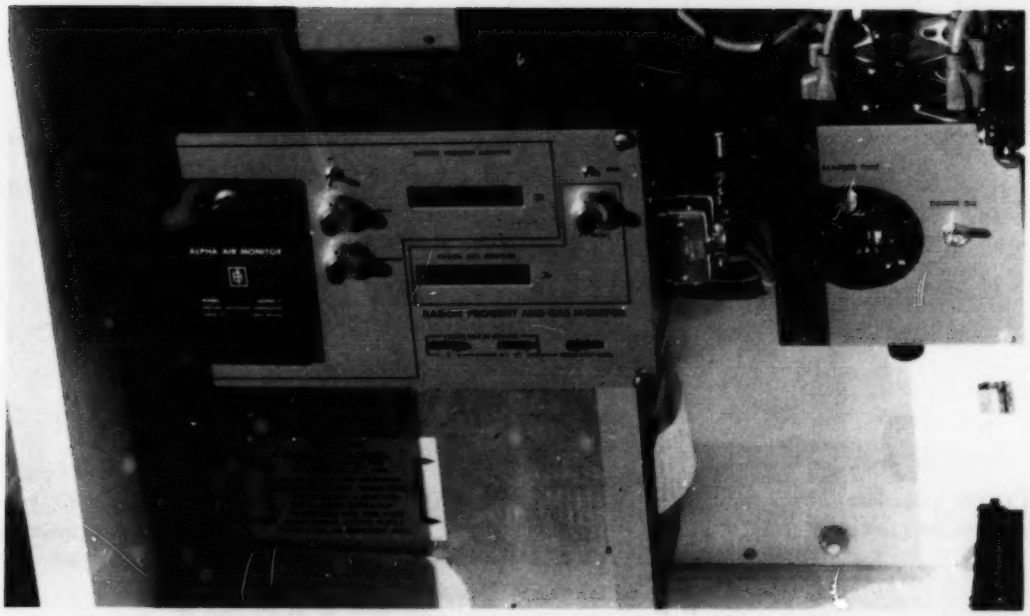

Figure 14. Photograph of CRWM-100.

Figure 15. CRWM-200 Enclosure.

Figure 16. CRWM-100 Enclosure.

for detection efficiency, the activities of radon-222, polonium-218, and polonium-214 are determined from the area under each peak.

THEORETICAL PREDICTION OF WORKING LEVEL

Figures 11 and 12 depict block diagrams of working-level monitors CRWM-200 and CRWM-100, respectively. A surface-barrier detector measures alpha activity emitted principally from polonium-218 and polonium-214 on the filter.

Buildup of radionuclides emitting alpha particles is given by the following differential equation for the growth of N_i on the filter:

$$dN_i/dt = \lambda_{i-1} N_{i-1} - \lambda_i N_i + \chi_i V \tag{39}$$

where χ_i = radon (i = 1) or daughter (i = 2 to 4) concentration in air in atoms per liter at time t,

N_i = number of atoms of i-th isotope collected on filter, and

V = sampling flow rate in liters per minute,

with the restraints $i > 1$ and $N_i = 0$ at $t = 0$. Because radon does not collect on the filter, $N_1 = 0$ at all times. The ingrowth of radon daughters in air is a function of radon transit time, τ, and decay constants, λ_i. The air concentration is given by:

$$\chi_i = \chi_1 \left(\prod_{j=1}^{i-1} \lambda_j \right) \sum_{j=1}^{i} \left[\frac{e^{-\lambda_j \tau}}{\prod_{\substack{k=1 \\ k \neq j}}^{i} (\lambda_k - \lambda_j)} \right] \tag{40}$$

thus for i = 3:

$$\chi_3 = \lambda_1 \lambda_2 \chi_1 \left[\frac{e^{-\lambda_1 \tau}}{(\lambda_2 - \lambda_1)(\lambda_3 - \lambda_1)} + \frac{e^{-\lambda_2 \tau}}{(\lambda_1 - \lambda_2)(\lambda_3 - \lambda_2)} + \frac{e^{-\lambda_3 \tau}}{(\lambda_1 - \lambda_3)(\lambda_2 - \lambda_3)} \right] \tag{41}$$

To model the working-level-monitor response under continuously varying concentrations, we have again assumed a sinusoidal radon concentration with concomitant daughter concentrations. Thus:

$$\chi_1 = \chi_1^0 (1 + a \sin kt) \tag{42}$$

where a and k were defined previously for the radon monitors and χ_1^0 is the mean radon concentration. Defining χ_i^0 as the value of χ_i with $\chi_1 = \chi_1^0$, Eq. 39 can be written as:

$$dN_i/dt = \lambda_{i-1} N_{i-1} - \lambda_i N_i + V \chi_i^0 (1 + a \sin kt) \tag{43}$$

If τ and χ_1^0 are constant, χ_i^0 is constant; then with V, a, and k also assumed constant, the solutions of Eq. 43 for i = 2 to 4 are simplified to:

$$N_2 = V \chi_2^0 \left[(1 - e^{-\lambda_2 \tau})/\lambda_2 + \frac{a}{\lambda_2^2 + k^2} (k e^{-\lambda_2 t} + \lambda_2 \sin kt - k \cos kt)\right] \tag{44}$$

$$N_3 = V (\chi_2^0 + \chi_3^0)/\lambda_3 + I_5 e^{-\lambda_3 t} + Q_5 e^{-\lambda_2 t}/(\lambda_3 - \lambda_2) + \frac{(Q_6 \lambda_3 - Q_7 k^2) \sin kt - k (Q_6 + \lambda_3 Q_7) \cos kt}{\lambda_3^2 + k^2} \tag{45}$$

where

$$Q_5 = V \chi_2^0 \left(\frac{a k \lambda_2}{\lambda_2^2 + k^2} - 1\right) \tag{46}$$

$$Q_6 = V a \left(\frac{\lambda_2^2 \chi_2^0}{\lambda_2^2 + k^2} + \chi_3^0\right) \tag{47}$$

$$Q_7 = V.a \lambda_2 \chi_2^0/(\lambda_2^2 + k^2) \tag{48}$$

$$I_5 = \frac{k (Q_6 + \lambda_3 Q_7)}{\lambda_3^2 + k^2} - \frac{V (\chi_2^0 + \chi_3^0)}{\lambda_3} - \frac{Q_5}{\lambda_3 - \lambda_2} \tag{49}$$

and

$$N_4 = \frac{V}{\lambda_4} (\chi_2^0 + \chi_3^0 + \chi_4^0) + I_6 e^{-\lambda_4 t} + \frac{I_5 \lambda_3 e^{-\lambda_3 t}}{\lambda_4 - \lambda_3} - \frac{(k Q_8 + \lambda_4 Q_9) \cos kt}{\lambda_4^2 + k^2} + \frac{(Q_8 \lambda_4 - k Q_9) \sin kt}{\lambda_4^2 + k^2} \tag{50}$$

where $$Q_8 = V\,a\,\chi_4^0 + \frac{\lambda_3\,(Q_6\,\lambda_3 - Q_7\,k^2)}{\lambda_3^2 + k^2} \tag{51}$$

$$Q_9 = \frac{\lambda_3\,k\,(Q_6 + \lambda_3\,Q_7)}{\lambda_3^2 + k^2} \tag{52}$$

$$I_6 = -\frac{V\,(\chi_2^0 + \chi_3^0 + \chi_4^0)}{\lambda_4} - \frac{I_5\,\lambda_3}{\lambda_4 - \lambda_3} - \frac{\lambda_3\,Q_5}{(\lambda_3 - \lambda_2)\,(\lambda_4 - \lambda_2)}$$

$$+ \frac{k\,Q_8 + \lambda_4\,Q_9}{\lambda_4^2 + k^2} \tag{53}$$

The time-integrated activity on the filter, A_i, is given by:

$$A_i = \int_{t_1}^{t_2} \lambda_i\,N_i\,dt \tag{54}$$

$$A_2 = V\,\chi_2^0\,[\Delta t + (\frac{1}{\lambda_2} - \frac{a\,k}{\lambda_2^2 + k_2^2})\,(\Delta e_2) - \frac{a\,\lambda_2}{\lambda_2^2 + k^2}\,(\frac{\lambda_2\,f_c}{k} + f_s)] \tag{55}$$

$$A_3 = V\,(\chi_2^0 + \chi_3^0)\,\Delta t + I_5\,\Delta e_3 + \frac{Q_5\,\lambda_3\,\Delta e_2}{(\lambda_3 - \lambda_2)\,\lambda_2}$$

$$- \frac{\lambda_3\,(Q_6\,\lambda_3 - Q_7\,k^2)\,f_c}{(\lambda_3^2 + k^2)\,k} - \frac{\lambda_3\,(Q_6 + \lambda_3\,Q_7)\,f_s}{\lambda_3^2 + k^2} \tag{56}$$

and $$A_4 = V\,(\chi_2^0 + \chi_3^0 + \chi_4^0)\,\Delta t + I_6\,\Delta e_4 + \frac{I_5\,\lambda_4\,\Delta e_3}{\lambda_4 - \lambda_3}$$

$$+ \frac{\lambda_3\,\lambda_4\,Q_5\,\Delta e_2}{(\lambda_3 - \lambda_2)\,(\lambda_4 - \lambda_2)\,\lambda_2} - \frac{\lambda_4\,(\lambda_4\,Q_8 - k\,Q_9)\,f_c}{(\lambda_4^2 + k^2)\,k}$$

$$- \frac{\lambda_4\,(k\,Q_8 + \lambda_4\,Q_9)\,f_s}{(\lambda_4^2 + k^2)\,k} \tag{57}$$

where $\Delta e_i = e^{-\lambda_i t_1} - e^{-\lambda_i t_2}$ (58)

From Eq. 40 and 42 we can write:

$$\lambda_i \chi_i \approx \lambda_i \chi_i^0 (1 + a \sin kt) \quad (59)$$

Air activities, $A_{i,air}$, are obtained by direct integration of Eq. 59 with the result:

$$A_{i,air} = \lambda_i \chi_i^0 (\Delta t - a f_c/k) \quad (60)$$

By definition, working level is:

$$WL = \sum_{i=2}^{4} L_i \chi_i = \sum_{i=2}^{4} L_i A_{i,air}/\lambda_i \quad (61)$$

where $$L_i = \frac{1}{1.3 \times 10^5} \sum_{i=2}^{4} E_i \quad (62)$$

where E_i is the alpha energy in MeV from Table 1. Working level can be correlated to the total observed alpha count on the filter by:

$$WL = f\ C/(60V\ E) \quad (63)$$

where f is the calculated conversion factor in (WL L)/dpm, C is the hourly count rate, 60V is the volume of air sampled during one hour, and E is the efficiency of the detector.

The conversion factors for polonium-218 and polonium-214 in air are 5.9×10^{-5} and 5.3×10^{-5}, respectively, based on the working-level definition of 1.3×10^5 MeV/(WL L). Because air contains both these radionuclides in amounts depending on the equilibrium conditions, an average f of 5.6×10^{-5} was used by Momeni et al. (1979b). The error associated with this choice is at most 5.4%.

Tables 10, 11, 12, and 13 present a comparison of "true" (Eq. 61) vs. "observed" (Eq. 63) working-level-monitor responses for various transit times and relative sine amplitudes, by hour and by day. They give hourly predicted concentrations of radon and its daughters and working levels for the first 24 hours after a new filter is installed, and 24-hour values for seven days of operation. Working levels were estimated from Eq. 61 and from activity on the filter. The differences between the true and observed values are also given in these tables. In all cases, $\lambda_1 \chi_1 e^{-\lambda_1 \tau} = 1$, $E_i = 1$, and V = 1 L/min were assumed. Thus, the "observed" total alpha count rate on the filter is $(A_2 + A_4)$.

Table 10. Time-Integrated Activities in Air (pCi/L), on Filter (pCi), and Working Levels by Hour and by Day (sine period = 24 h, relative amplitude = 0.5, transit time = 0.1 h)

	In Air				On Filter			Working Level		
Hour	Rn-222	Po-218	Pb-214	Bi-214	Po-218	Pb-214	Bi-214	True	Observed	Obs.- True
1	1.065077	0.792921	0.070992	0.005293	3.69580	2.82350	1.05098	8.970E-006	4.430E-006	-4.540E-006
2	1.190796	0.886515	0.079371	0.005917	3.87167	5.84661	4.73209	1.003E-005	8.030E-006	-1.999E-006
3	1.303512	0.970429	0.086884	0.006477	4.24487	7.04162	6.61836	1.098E-005	1.014E-005	-8.390E-007
4	1.395545	1.038945	0.093019	0.006935	4.55203	7.76176	7.59810	1.175E-005	1.134E-005	-4.130E-007
5	1.460622	1.087393	0.097356	0.007258	4.77222	8.26837	8.22899	1.230E-005	1.213E-005	-1.667E-007
6	1.494308	1.112472	0.099602	0.007425	4.89043	8.59270	8.64997	1.258E-005	1.264E-005	5.286E-008
7	1.494308	1.112472	0.099602	0.007425	4.89861	8.72658	8.87694	1.258E-005	1.286E-005	2.723E-007
8	1.460622	1.087393	0.097356	0.007258	4.79621	8.66383	8.90459	1.230E-005	1.279E-005	4.863E-007
9	1.395545	1.038945	0.093019	0.006935	4.59019	8.40935	8.73329	1.175E-005	1.244E-005	6.822E-007
10	1.303512	0.970429	0.086884	0.006477	4.29460	7.98063	8.37519	1.098E-005	1.183E-005	8.471E-007
11	1.190796	0.886515	0.079371	0.005917	3.92959	7.40690	7.85480	1.003E-005	1.100E-005	9.700E-007
12	1.065077	0.792921	0.070992	0.005293	3.52002	6.72728	7.20760	8.970E-006	1.001E-005	1.043E-006
13	0.934923	0.696025	0.062316	0.004646	3.09382	5.98807	6.47772	7.874E-006	8.933E-006	1.060E-006
14	0.809204	0.602431	0.053937	0.004021	2.68002	5.23965	5.71488	6.815E-006	7.835E-006	1.020E-006
15	0.696488	0.518516	0.046424	0.003461	2.30682	4.53303	4.97108	5.866E-006	6.793E-006	9.270E-007
16	0.604455	0.450000	0.040289	0.003004	1.99966	3.91636	4.29700	5.091E-006	5.877E-006	7.862E-007
17	0.539378	0.401552	0.035952	0.002680	1.77947	3.43167	3.73858	4.543E-006	5.150E-006	6.076E-007
18	0.505692	0.376474	0.033706	0.002513	1.66126	3.11199	3.33388	4.259E-006	4.662E-006	4.033E-007
19	0.505692	0.376474	0.033706	0.002513	1.65307	2.97910	3.11048	4.259E-006	4.446E-006	1.871E-007
20	0.539378	0.401552	0.035952	0.002680	1.75548	3.04206	3.08359	4.543E-006	4.516E-006	-2.610E-008
21	0.604455	0.450000	0.040289	0.003004	1.96150	3.29657	3.25506	5.091E-006	4.869E-006	-2.218E-007
22	0.696488	0.518516	0.046424	0.003461	2.25708	3.72530	3.61320	5.866E-006	5.479E-006	-3.868E-007
23	0.809204	0.602431	0.053937	0.004021	2.62210	4.29903	4.13360	6.815E-006	6.305E-006	-5.097E-007
24	0.934923	0.696025	0.062316	0.004646	3.03166	4.97866	4.78079	7.874E-006	7.292E-006	-5.822E-007

	In Air				On Filter			Working Level		
Day	Rn-222	Po-218	Pb-214	Bi-214	Po-218	Pb-214	Bi-214	True	Observed	Obs.- True
1	1.000000	0.744473	0.066654	0.004969	3.28576	5.69961	5.72253	8.422E-006	8.408E-006	-1.412E-008
2	1.000000	0.744473	0.066654	0.004969	3.27584	5.85297	5.99420	8.422E-006	8.652E-006	2.302E-007
3	1.000000	0.744473	0.066654	0.004969	3.27584	5.85297	5.99420	8.422E-006	8.652E-006	2.302E-007
4	1.000000	0.744473	0.066654	0.004969	3.27584	5.85297	5.99420	8.422E-006	8.652E-006	2.302E-007
5	1.000000	0.744473	0.066654	0.004969	3.27584	5.85297	5.99420	8.422E-006	8.652E-006	2.302E-007
6	1.000000	0.744473	0.066654	0.004969	3.27584	5.85297	5.99420	8.422E-006	8.652E-006	2.302E-007
7	1.000000	0.744473	0.066654	0.004969	3.27584	5.85297	5.99420	8.422E-006	8.652E-006	2.302E-007

Table 11. Time-Integrated Activities in Air (pCi/L), on Filter (pCi), and Working Levels by Hour and by Day (sine period = 24 h, relative amplitude = 0.5, transit time = 1.0 h)

	In Air				On Filter			Working Level		
Hour	Rn-222	Po-218	Pb-214	Bi-214	Po-218	Pb-214	Bi-214	True	Observed	Obs.- True
1	1.065077	1.065666	0.813070	0.529765	4.96707	17.23686	14.52553	5.400E-005	1.819E-005	-3.581E-005
2	1.190796	1.191455	0.909042	0.592297	5.20343	34.20134	42.31287	6.038E-005	4.435E-005	-1.603E-005
3	1.303512	1.304234	0.995089	0.648361	5.70500	40.96891	55.16319	6.609E-005	5.681E-005	-9.281E-006
4	1.395545	1.396317	1.065346	0.694138	6.11782	45.09106	62.17298	7.076E-005	6.374E-005	-7.019E-006
5	1.460622	1.461430	1.115025	0.726507	6.41375	47.99315	66.83035	7.406E-005	6.836E-005	-5.696E-006
6	1.494308	1.495135	1.140741	0.743262	6.57262	49.83891	69.88271	7.577E-005	7.136E-005	-4.407E-006
7	1.494308	1.495135	1.140741	0.743262	6.58362	50.57913	71.37485	7.577E-005	7.276E-005	-3.004E-006
8	1.460622	1.461430	1.115025	0.726507	6.44599	50.17960	71.26192	7.406E-005	7.253E-005	-1.530E-006
9	1.395545	1.396317	1.065346	0.694138	6.16911	48.67099	69.56408	7.076E-005	7.068E-005	-7.323E-008
10	1.303512	1.304234	0.995089	0.648361	5.77185	46.15683	66.39970	6.609E-005	6.736E-005	1.269E-006
11	1.190796	1.191455	0.909042	0.592297	5.28128	42.80861	61.98501	6.038E-005	6.278E-005	2.406E-006
12	1.065077	1.065666	0.813070	0.529765	4.73083	38.85454	56.62099	5.400E-005	5.726E-005	3.260E-006
13	0.934923	0.935441	0.713712	0.465027	4.15802	34.56409	50.67322	4.740E-005	5.118E-005	3.773E-006
14	0.809204	0.809652	0.617739	0.402495	3.60188	30.22964	44.54701	4.103E-005	4.494E-005	3.910E-006
15	0.696488	0.696873	0.531692	0.346430	3.10031	26.14660	38.65988	3.531E-005	3.898E-005	3.663E-006
16	0.604455	0.604790	0.461436	0.300653	2.68750	22.59319	33.41302	3.065E-005	3.369E-005	3.046E-006
17	0.539378	0.539677	0.411756	0.268284	2.39157	19.81160	29.16399	2.735E-005	2.945E-005	2.104E-006
18	0.505692	0.505972	0.386041	0.251529	2.23269	17.99137	26.20236	2.564E-005	2.654E-005	8.996E-007
19	0.505692	0.505972	0.386041	0.251529	2.22169	17.25655	24.72996	2.564E-005	2.515E-005	-4.850E-007
20	0.539378	0.539677	0.411756	0.268284	2.35932	17.65723	24.84713	2.735E-005	2.539E-005	-1.955E-006
21	0.604455	0.604790	0.461436	0.300653	2.63620	19.16608	26.54588	3.065E-005	2.724E-005	-3.411E-006
22	0.696488	0.696873	0.531692	0.346430	3.03347	21.68030	29.71045	3.531E-005	3.056E-005	-4.753E-006
23	0.809204	0.809652	0.617739	0.402495	3.52404	25.02853	34.12518	4.103E-005	3.514E-005	-5.889E-006
24	0.934923	0.935441	0.713712	0.465027	4.07448	28.98260	39.48921	4.740E-005	4.066E-005	-6.743E-006

	In Air				On Filter			Working Level		
Day	Rn-222	Po-218	Pb-214	Bi-214	Po-218	Pb-214	Bi-214	True	Observed	Obs.- True
1	1.000000	1.000554	0.763391	0.497396	4.41598	33.07032	46.25840	5.070E-005	4.730E-005	-3.406E-006
2	1.000000	1.000554	0.763391	0.497396	4.40266	33.91857	48.05510	5.070E-005	4.896E-005	-1.742E-006
3	1.000000	1.000554	0.763391	0.497396	4.40266	33.91857	48.05510	5.070E-005	4.896E-005	-1.742E-006
4	1.000000	1.000554	0.763391	0.497396	4.40266	33.91857	48.05510	5.070E-005	4.896E-005	-1.742E-006
5	1.000000	1.000554	0.763391	0.497396	4.40266	33.91857	48.05510	5.070E-005	4.896E-005	-1.742E-006
6	1.000000	1.000554	0.763391	0.497396	4.40266	33.91857	48.05510	5.070E-005	4.896E-005	-1.742E-006
7	1.000000	1.000554	0.763391	0.497396	4.40266	33.91857	48.05510	5.070E-005	4.896E-005	-1.742E-006

Table 12. Time-Integrated Activities in Air (pCi/L), on Filter (pCi), and Working Levels by Hour and by Day (sine period = 24 h, relative amplitude = 0.5, transit time = 10.0 h)

	In Air				On Filter			Working Level		
Hour	Rn-222	Po-218	Pb-214	Bi-214	Po-218	Pb-214	Bi-214	True	Observed	Obs.- True
1	1.065077	1.065668	1.070885	1.074733	4.96708	22.06589	24.83539	7.907E-005	2.782E-005	-5.125E-005
2	1.190796	1.191456	1.197289	1.201592	5.20344	43.66516	65.53506	8.840E-005	6.602E-005	-2.238E-005
3	1.303512	1.304235	1.310620	1.315330	5.70501	52.28697	83.64735	9.677E-005	8.340E-005	-1.337E-005
4	1.395545	1.396319	1.403155	1.408197	6.11782	57.54228	93.72459	1.036E-004	9.319E-005	-1.041E-005
5	1.460622	1.461432	1.468587	1.473864	6.41375	61.24233	100.49882	1.084E-004	9.979E-005	-8.646E-006
6	1.494308	1.495137	1.502457	1.507856	6.57263	63.59458	104.90780	1.109E-004	1.040E-004	-6.883E-006
7	1.494308	1.495137	1.502457	1.507856	6.58363	64.53608	106.97801	1.109E-004	1.060E-004	-4.941E-006
8	1.460622	1.461432	1.468587	1.473864	6.44600	64.02333	106.64130	1.084E-004	1.055E-004	-2.883E-006
9	1.395545	1.396319	1.403155	1.408197	6.16912	62.09562	103.93653	1.036E-004	1.028E-004	-8.346E-007
10	1.303512	1.304235	1.310620	1.315330	5.77185	58.88525	99.05144	9.677E-005	9.784E-005	1.067E-006
11	1.190796	1.191456	1.197289	1.201592	5.28128	54.61120	92.31968	8.840E-005	9.109E-005	2.694E-006
12	1.065077	1.065668	1.070885	1.074733	4.73083	49.56479	84.20016	7.907E-005	8.300E-005	3.935E-006
13	0.934923	0.935442	0.940021	0.943399	4.15802	44.08992	75.24624	6.941E-005	7.411E-005	4.706E-006
14	0.809204	0.809653	0.813617	0.816541	3.60188	38.55970	66.06813	6.007E-005	6.503E-005	4.953E-006
15	0.696488	0.696874	0.700286	0.702802	3.10031	33.35100	57.29131	5.170E-005	5.637E-005	4.661E-006
16	0.604455	0.604791	0.607751	0.609935	2.68750	28.81880	49.51389	4.487E-005	4.872E-005	3.849E-006
17	0.539378	0.539678	0.542320	0.544268	2.39157	25.27195	43.26590	4.004E-005	4.261E-005	2.572E-006
18	0.505692	0.505973	0.508450	0.510277	2.23269	22.95216	38.97312	3.754E-005	3.846E-005	9.181E-007
19	0.505692	0.505973	0.508450	0.510277	2.22169	22.01753	36.92811	3.754E-005	3.654E-005	-1.001E-006
20	0.539378	0.539678	0.542320	0.544268	2.35933	22.53174	37.27023	4.004E-005	3.699E-005	-3.054E-006
21	0.604455	0.604791	0.607751	0.609935	2.63621	24.45976	39.97615	4.487E-005	3.977E-005	-5.101E-006
22	0.696488	0.696874	0.700286	0.702802	3.03347	27.67019	44.86149	5.170E-005	4.470E-005	-7.003E-006
23	0.809204	0.809653	0.813617	0.816541	3.52404	31.94425	51.59330	6.007E-005	5.144E-005	-8.629E-006
24	0.934923	0.935442	0.940021	0.943399	4.07449	36.99067	59.71283	6.941E-005	5.953E-005	-9.870E-006

	In Air				On Filter			Working Level		
Day	Rn-222	Po-218	Pb-214	Bi-214	Po-218	Pb-214	Bi-214	True	Observed	Obs.- True
1	1.000000	1.000555	1.005453	1.009066	4.41599	42.19880	69.45737	7.424E-005	6.895E-005	-5.288E-006
2	1.000000	1.000555	1.005453	1.009066	4.40266	43.27773	71.95650	7.424E-005	7.127E-005	-2.968E-006
3	1.000000	1.000555	1.005453	1.009066	4.40266	43.27773	71.95650	7.424E-005	7.127E-005	-2.968E-006
4	1.000000	1.000555	1.005453	1.009066	4.40266	43.27773	71.95650	7.424E-005	7.127E-005	-2.968E-006
5	1.000000	1.000555	1.005453	1.009066	4.40266	43.27773	71.95650	7.424E-005	7.127E-005	-2.968E-006
6	1.000000	1.000555	1.005453	1.009066	4.40266	43.27773	71.95650	7.424E-005	7.127E-005	-2.968E-006
7	1.000000	1.000555	1.005453	1.009066	4.40266	43.27773	71.95650	7.424E-005	7.127E-005	-2.968E-006

Table 13. Time-Integrated Activities in Air (pCi/L), on Filter (pCi), and Working Levels by Hour and by Day (sine period = 24 h, relative amplitude = 1.0, transit time = 1.0 h)

	In Air				On Filter			Working Level		
Hour	Rn-222	Po-218	Pb-214	Bi-214	Po-218	Pb-214	Bi-214	True	Observed	Obs.- True
1	1.130154	1.130779	0.862749	0.562134	5.20861	18.02739	12.88454	5.730E-005	1.689E-005	-4.041E-005
2	1.381592	1.382356	1.054694	0.687198	6.00421	38.19459	46.43138	7.005E-005	4.894E-005	-2.111E-005
3	1.607024	1.607914	1.226788	0.799327	7.00734	48.80536	64.73659	8.148E-005	6.696E-005	-1.452E-005
4	1.791090	1.792081	1.367301	0.890880	7.83298	56.43009	76.85873	9.081E-005	7.905E-005	-1.177E-005
5	1.921243	1.922307	1.466659	0.955618	8.42483	62.10301	85.73143	9.741E-005	8.788E-005	-9.533E-006
6	1.988616	1.989717	1.518091	0.989129	8.74259	65.76672	91.73765	1.008E-004	9.378E-005	-7.044E-006
7	1.988616	1.989717	1.518091	0.989129	8.76459	67.24127	94.70047	1.008E-004	9.657E-005	-4.260E-006
8	1.921243	1.922307	1.466659	0.955618	8.48932	66.44097	94.47000	9.741E-005	9.610E-005	-1.316E-006
9	1.791090	1.792081	1.367301	0.890880	7.93556	63.42348	91.07332	9.081E-005	9.241E-005	1.596E-006
10	1.607024	1.607914	1.226788	0.799327	7.14104	58.39510	84.74436	8.148E-005	8.576E-005	4.280E-006
11	1.381592	1.382356	1.054694	0.687198	6.15990	51.69845	75.91494	7.005E-005	7.660E-005	6.553E-006
12	1.130154	1.130779	0.862749	0.562134	5.05900	43.79050	65.18689	5.730E-005	6.556E-005	8.261E-006
13	0.869846	0.870328	0.664033	0.432658	3.91338	35.20960	53.29133	4.410E-005	5.339E-005	9.288E-006
14	0.618408	0.618751	0.472087	0.307594	2.80110	26.54072	41.03898	3.135E-005	4.092E-005	9.568E-006
15	0.392976	0.393193	0.299994	0.195464	1.79797	18.37462	29.26467	1.992E-005	2.899E-005	9.067E-006
16	0.208910	0.209026	0.159480	0.103911	0.97234	11.26782	18.77094	1.059E-005	1.843E-005	7.835E-006
17	0.078757	0.078800	0.060122	0.039173	0.38048	5.70463	10.27289	3.993E-006	9.943E-006	5.950E-006
18	0.011384	0.011390	0.008690	0.005662	0.06272	2.06417	4.34962	5.772E-007	4.118E-006	3.541E-006
19	0.011384	0.011390	0.008690	0.005662	0.04073	0.59454	1.40482	5.772E-007	1.349E-006	7.720E-007
20	0.078757	0.078800	0.060122	0.039173	0.31599	1.39589	1.63915	3.993E-006	1.825E-006	-2.168E-006
21	0.208910	0.209026	0.159480	0.103911	0.86975	4.41360	5.03666	1.059E-005	5.513E-006	-5.080E-006
22	0.392976	0.393193	0.299994	0.195464	1.66428	9.44202	11.36580	1.992E-005	1.216E-005	-7.763E-006
23	0.618408	0.618751	0.472087	0.307594	2.64542	16.13849	20.19525	3.135E-005	2.132E-005	-1.004E-005
24	0.869846	0.870328	0.664033	0.432658	3.74631	24.04663	30.92331	4.410E-005	3.236E-005	-1.175E-005

	In Air				On Filter			Working Level		
Day	Rn-222	Po-218	Pb-214	Bi-214	Po-218	Pb-214	Bi-214	True	Observed	Obs.- True
1	1.000000	1.000554	0.763391	0.497396	4.41585	33.14624	47.33432	5.070E-005	4.737E-005	-3.336E-006
2	1.000000	1.000554	0.763391	0.497396	4.40266	33.91857	48.05510	5.070E-005	4.896E-005	-1.742E-006
3	1.000000	1.000554	0.763391	0.497396	4.40266	33.91857	48.05510	5.070E-005	4.896E-005	-1.742E-006
4	1.000000	1.000554	0.763391	0.497396	4.40266	33.91857	48.05510	5.070E-005	4.896E-005	-1.742E-006
5	1.000000	1.000554	0.763391	0.497396	4.40266	33.91857	48.05510	5.070E-005	4.896E-005	-1.742E-006
6	1.000000	1.000554	0.763391	0.497396	4.40266	33.91857	48.05510	5.070E-005	4.896E-005	-1.742E-006
7	1.000000	1.000554	0.763391	0.497396	4.40266	33.91857	48.05510	5.070E-005	4.896E-005	-1.742E-006

As it was observed for radon, the lag-time error produced by a periodic concentration change is about proportional to the cycle amplitude (Tables 10, 11, 12, and 13). After the first five hours, the worst-case error in the hourly data is about 23% of the daily mean. The 24-hour averages are of interest in that they show a fixed error (after the first day) dependent only on the transit time. This is a direct consequence of the fixed value of the conversion factor f used in Eq. 63. Clearly, a better choice for f could be made on the basis of a location-dependent transit time (distance divided by average wind speed). Figure 17 gives the correct value of f as a function of transit time. The choice of $f = 5.6 \times 10^{-5}$ corresponds to the estimated transient time for monitoring stations in the vicinity of the sources of release. For ambient measurements of working level, a larger conversion factor (e.g. about 5.8×10^{-5}) is recommended.

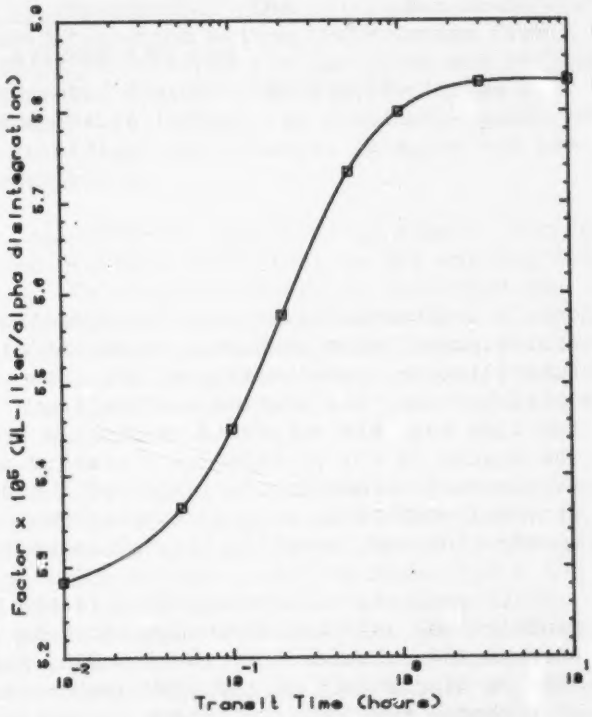

Figure 17.

Working-Level Conversion Factor.

TYPICAL OPERATION OF THE CRWM SYSTEM

Figure 18 shows typical radon-concentration and working-level data as a function of time, measured at the Anaconda Uranium Mill, using a CRWM-100 system. In general, faster radon-concentration variations are damped out in the working-level profile by dispersion of radon daughters in the atmosphere. The profile of working level conforms to that of radon concentration.

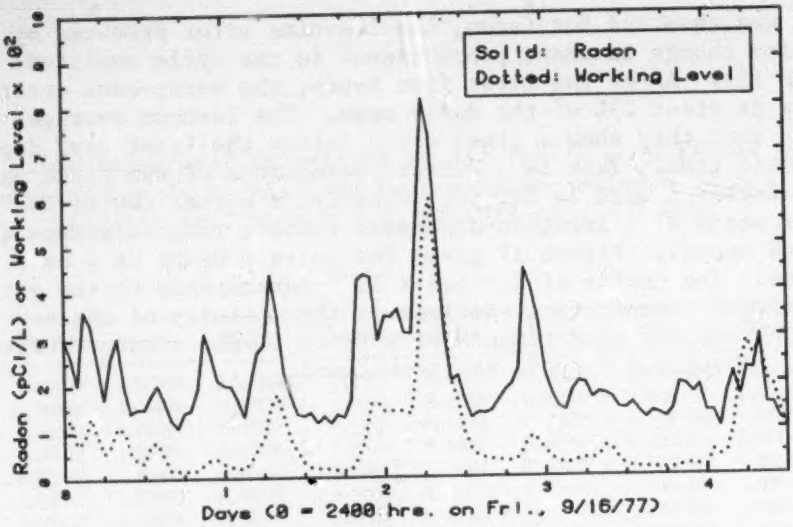

Figure 18. Typical Radon Concentration and Working Level at the Anaconda Uranium Mill, Station 103.

A recommended procedure for operation of the CRWM system is to change the filter paper twice each week depending on the amount of airborne particulates. Scintillation cells usually do not show a reduction in sensitivity or increase in background, but routine calibrations for radon, alpha detectors, leakage, and flow rate are suggested as monthly procedures. Continuous operation of the system in the vicinity of a uranium mine or mill may require replacement of the surface-barrier detector and the radon cell twice each year. Under abnormal conditions such as dust storms, the system will require immediate examination and, specifically, cleaning of the surface-barrier detector.

In general, filter papers collected from the CRWM system may be composited monthly and analyzed after chemical separation of the long-lived radionuclides, uranium-238, uranium-234, thorium-230, radium-226, lead-210, and polonium-210. Thus, a single unit of the CRWM system can be used for a complete monitoring of airborne particulates, radon concentration, and working level.

SUMMARY

Techniques for measurement of radon concentration in air and working level are reviewed with emphasis toward routine monitoring of ambient air and application within industrial environments. Field conditions are unlike the controlled moisture, temperature, and dust environment of a research laboratory. Equipment designed for the field must be rugged and reasonably insensitive to the above parameters. In addition, an accuracy of ± 20% or better over the entire range of measurement is often demanded. Equipment sensitivity must be lower than the lowest ambient concentration. The techniques of measurement of

radon and working level are broadly divided into grab-sample, integrating, and continuous-measurement methods.

The grab-sample method, using brief periods of sample collection, cannot provide reliable estimates of radon concentration in the free atmosphere due to large temporal atmospheric variations. For the same reason, instantaneous measurement of working level should not be applied to dynamic and variable free-air environments for estimation of the average working level. However, under static conditions of air movement, such as closed spaces, the grab-sample method may provide estimates of average radon concentration in air and working level.

Both integrating and continuous-measurement methods provide reliable estimates of the average concentration of radon in air. Among the integrating methods, those that do not require correction of radon concentration in air provide a more reliable estimation of the average. The continuous-measurement method, using any predetermined time-integration period, may provide from nearly instantaneous to long time averages of radon concentration and working level. In addition, systems designed with microprocessor capabilities are able to provide online summaries of the data. Thus, the continuous-measurement method is also a valuable tool for recording of accidental releases and concentration under abnormal weather conditions.

The systems CRM-100, CRWM-100, and CRWM-200 developed by Argonne National Laboratory for continuous measurement of radon concentration and working level under field conditions are described. Calibration theory is developed and diurnal variation of radon concentration in air is simulated using a sinusoidal radon concentration. Under simulated conditions and assuming the worst case, the maximum hourly error is only about 10% of the mean radon activity, but the error within a single cycle period averages to zero. Under these conditions, the simulation indicates the actual input data.

The calibration factor for radon-222, which is determined by the detection of polonium-218 and polonium-214 and includes the deposition factor, is studied as a function of ambient pressure, temperature, and humidity changes. Operation of the radon monitor under ambient-temperature changes (240 K to 315 K) and pressure changes (90 to 100 kPa) produces a calibration-factor variation of about 7%. Calibration factor is independent of moisture up to 70% relative humidity. It shows dependence on airflow rate for the system investigated: 4.19 cpm/(pCi/L) under static conditions (no flow through the detector) and 3.5 cpm/(pCi/L) for a 5-L/min flow rate. Because ambient concentrations are usually less than 1 pCi/L, the system sensitivity is studied at low radon concentrations; it is a very linear function of radon concentration up to 1 pCi/L. Under laboratory conditions, radon concentration in air as low as 0.05 pCi/L may be detected.

Determination of working level (WL), from the combined alpha counts from polonium-218 and polonium-214, requires a knowledge of the relative equilibrium value between these two radionuclides. The calibration factor, i.e. WL per count per minute of the alphas, is calculated as a function of the transit time from the source to the detector. If the corrections for detection efficiency and flow rate are excluded, the calibration factor is 5.9×10^{-5} WL/dpm for polonium-218 and 5.3×10^{-5} WL/dpm for polonium-214. The error associated

with a choice of an average calibration factor of 5.6×10^{-5} (WL L)/dpm, corresponding to a transit time of about 15 minutes, is 5.4%. The function of the working-level system is simulated using a sinusoidal variation of ambient radon concentration. Because of the lag time, the worst-case error in the estimated hourly data is 23% of the daily mean. The 24-hour average shows a fixed error that is dependent on transit time. Considering these errors, a typical four-day measurement of radon concentration and working level at a site adjacent to the Anaconda Uranium Mill, Bluewater, New Mexico, indicates a variation in radon concentration from about 1 pCi/L to 8.2 pCi/L, an eightfold range. During the same period, the working level varies from 3×10^{-3} WL to 6×10^{-2} WL, a 20-fold range.

Based on intensive experience with these continuous monitors (Momeni et al. 1979b), and those manufactured for our field studies by the Eberline Instrument Corporation, we believe that these systems--with some modifications--may provide a reliable and comprehensive data base and serve well both for research and for routine ambient monitoring applications.

REFERENCES

Breslin, A.J., A.C. George, and M.S. Weinstein. 1969. "Investigation of the Radiological Characteristics of Uranium Mine Atmosphere." Health and Safety Laboratory, HASL-220, USAEC, New York Operations Office, New York City.

Budnitz, R.J. 1974. "Radon-222 and Its Daughters - A Review of Instrumentation for Occupational and Environmental Monitoring." Health Phys. 26:145-163.

Costa-Ribeiro, C., J. Thomas, R.T. Drew, M.E. Wrenn, and M. Eisenbud. 1969. "A Radon Daughter Suitable for Personnel or Area Monitoring." Health Phys. 17:193-198.

Curtis, L.F. 1942. "Prevention and Control of Hazards in the Radium Dial Painting Industry." J. Ind. Hyg. Toxicol. 24:131-141.

Dalu, G.A., and G. Dalu. 1969. "Scintillation Counter for the Direct Measurement of Radon Concentration." Atti Conv. Geofis. Ital. XVIII, Part II, pp. 791-803.

Dalu, G.A., and G. Dalu. 1971. "An Automatic Counter for Direct Measurements of Radon Concentration." Aerosol Sci. 2:247-255.

Evans, R.D. 1955. "The Atomic Nucleus." McGraw-Hill Book Company, Inc., New York City.

Geiger, Eric L. 1967. "Radon Film Badge." Health Phys. 13:407-411.

George, A.C., A.J. Breslin, and S.F. Guggenheim. 1976. "A Cumulative Environmental Radon Monitor." Proc. Ninth Midyear Health Phys. Symp., Denver, CO.

George, A.C., and A.J. Breslin. 1977. "Measurements of Environmental Radon with Integrating Instruments." Workshop on Methods for Measuring Radiation in and Around Uranium Mills 3(9), E.D. Harward, ed., Atomic Industrial Forum, Inc.

Groer, P.G., R.D. Evans, and D.A. Gordon. 1972. "Accuracy and Precision of the Kusnetz Method for the Determination of the Working Level in Uranium Mines." Health Phys. 24:106.

Harris, W.B., H.D. LeVine, and S.I. Watnick. 1957. "Portable Radon Detectors for Continuous Air Monitoring." AMA Arch. Ind. Health 16(6):493-498.

Hill, A. 1975. "Rapid Measurement of Radon, Decay Products, Unattached Fractions, and Working Level Values of Mine Atmospheres." Health Phys. 28:472.

Holub, R.F., and R.F. Droullard. 1977. "Evaluation of Various Radon Daughter Measurement Methods." Workshop on Methods for Measuring Radiation in and Around Uranium Mills 3(9), E.D. Harward, ed., Atomic Industrial Forum, Inc.

Hursh, J.R. 1954. "Measurements of Breath Radon by Charcoal Adsorption." Nucleonics 12:62.

Kusnetz, H.L. 1956. "Radon Daughters in Mine Atmospheres - A Field Method for Determining Concentrations." Am. Ind. Hyg. Assoc. J. 17:85-88.

Lucas, H.F. 1957. "Improved Low-Level Alpha Scintillation Counters for Radon." Rev. Sci. Instrum. 28:680.

McLaughlin, J.P., and P.J. Nolan. 1969. "Detection of Radon in the Atmosphere." Proc. R. Ir. Acad. Sect. A 68(6):55.

Miller, R.W., J. Cleveland, and D. Kump. 1976. "An Instant Working Level Meter." Am. Ind. Hyg. Conf., Atlanta, GA.

Momeni, M.H., L.S. Rosenblatt, and N. Jow. 1976. "Retention and Distribution of Ra-226 in Beagles." Health Phys. 30:369.

Momeni, M.H., W.E. Kisieleski, Y. Yuan, and C.J. Roberts. 1978. "Radiological and Environmental Studies at Uranium Mills: A Comparison of Theoretical and Experimental Data." Presented at the Seminar on Management, Stabilization and Environmental Impact of Uranium Mill Tailings, Albuquerque, NM, organized by the OECD Nuclear Energy Agency.

Momeni, M.H., W.E. Kisieleski, S. Tyler, A. Zielen, Y. Yuan, and C.J. Roberts. 1979a. "Radiological Impact of Uranium Tailings and Alternatives for Their Management." Proceedings of the Health Physics Society 12th Midyear Topical Symposium, "Low-Level Radioactive Waste Management," U.S. Environmental Protection Agency 520/3-79-002.

Momeni, M.H., J.B. Lindstrom, C.E. Dungey, and W.E. Kisieleski. 1979b. "Radon and Radon-Daughter Concentrations in Air in the Vicinity of the Anaconda Uranium Mill." USNRC, NUREG/CR-1133, Argonne National Laboratory, ANL/ES-81.

Moses, H., H.F. Lucas, and G.A. Zerbe. 1963. "The Effect of Meteorological Variables upon Radon Concentration Three Feet Above the Ground." J. Air Pollut. Control Assoc. 13(1):12-19.

Shearer, S.D., and W.C. Sill. 1969. "Evaluation of Atmospheric Radon in the Vicinity of Uranium Mill Tailings." Health Phys. 17:77-88.

Sill, W.C., and S.D. Shearer. 1969. "Separation and Radiochemical Determination of Uranium and the Transuranium Elements Using Barium Sulfate." Health Phys. 17:89-107.

Thomas, J.W., and P.C. LeClare. 1970. "A Study of the Two-Filter Method for Radon-222." Health Phys. 18:113-122.

Thomas, J.W. 1972. "Measurement of Radon Daughters in Air." Health Phys. 23:483.

Van Dilla, M.A., and D.H. Taysum. 1955. "Scintillation Counter for Assay of Radon Gas." Nucleonics 13(2):68-69.

Wrenn, M.E., and H.B. Spitz. 1977. "The Design and Application of a Continuous Digital-Readout, Radon Measuring Instrument." Workshop on Methods for Measuring Radiation in and Around Uranium Mills 3(9), E.D. Harward, ed., Atomic Industrial Forum, Inc.

Distribution of NUREG/CR-1412 (ANL/ES-88)

Internal:

G.D. Ansley
A.J. Dvorak
D. Grahn
P.F. Gustafson
W.J. Hallett
R.B. Holtzman
R.B. Keener
W.E. Kisieleski (2)
J.H. Kittel
N.D. Kretz
J.H. Martens
W.E. Massey
J.E. Miranda
M.H. Momeni (12)
G.L. Montet
A.E. Packard
C.J. Roberts
W.K. Sinclair
A.F. Stehney
A.J. Zielen
ANL Contract File
ANL Libraries (5)
TIS Files (6)

External:

USNRC, for distribution per RU (343)
DOE-TIC (2)
Manager, Chicago Operations and Regional Office, DOE
Chief, Office of Patent Counsel, DOE-CORO
President, Argonne Universities Association
Abyss, J., United Nuclear - Homestake Partners, P.O. Box 3951, Albuquerque, NM 87110
Beverly, R.G., Union Carbide Corp., P.O. Box 1029, Grand Junction, CO 81501
Breslin, A.J., Environmental Measurements Lab., USDOE, New York, NY 10014
Geiger, E., Eberline Co., Santa Fe, NM 87501
Phillips, C.R., Univ. of Toronto, Dept. of Chemical Engineering, Toronto, Ontario, Canada M5S 1A4
Range, D., Exxon Minerals Co., P.O. Box 3020, Casper, WY 82602

NRC FORM 335 (7-77)

U.S. NUCLEAR REGULATORY COMMISSION

BIBLIOGRAPHIC DATA SHEET

1. REPORT NUMBER (Assigned by DDC): NUREG-CR-1412

4. TITLE AND SUBTITLE (Add Volume No., if appropriate): Systems for Continuous Measurement of Airborne Radon-222 Concentration and Working Levels

2. (Leave blank)

3. RECIPIENT'S ACCESSION NO.

7. AUTHOR(S): Michael A. Momeni, Albin J. Zielen, James E. Miranda, Jr., Norbert D. Kretz, Walter E. Kisieleski

5. DATE REPORT COMPLETED: MONTH April, YEAR 1980

9. PERFORMING ORGANIZATION NAME AND MAILING ADDRESS (Include Zip Code)

Argonne National Laboratory
9700 South Cass Avenue
Argonne, ILL 60439

DATE REPORT ISSUED: MONTH May, YEAR 1980

6. (Leave blank)

8. (Leave blank)

12. SPONSORING ORGANIZATION NAME AND MAILING ADDRESS (Include Zip Code)

Office of Nuclear Regulatory Research
U. S. Nuclear Regulatory Commission
Washington, D. C. 20555

10. PROJECT/TASK/WORK UNIT NO.

11. CONTRACT NO.: NRC FIN No. A2209

13. TYPE OF REPORT

PERIOD COVERED (Inclusive dates)

15. SUPPLEMENTARY NOTES

14. (Leave blank)

16. ABSTRACT (200 words or less)

The Argonne National Laboratory, under contract with the U. S. Nuclear Regulatory Commission (USNRC), has conducted extensive long-term field studies at operating uranium mills to provide input for the Generic Environmental Impact Statement on Uranium Milling being prepared by the USNRC.

As part of this broad field study, this report describes the design and calibration of a continuous radon and working level monitor. Particular note is given to those factors affecting accuracy and precision. The report further gives an overview of the techniques that have been developed for measuring radon and its daughters in air. Emphasis is on measurements for surveillance and protection in occupational and environmental situations.

17. KEY WORDS AND DOCUMENT ANALYSIS

17a. DESCRIPTORS

17b. IDENTIFIERS OPEN-ENDED TERMS

18. AVAILABILITY STATEMENT: Unlimited

19. SECURITY CLASS (This report): Unclassified

20. SECURITY CLASS (This page): Unclassified

21. NO. OF PAGES

22. PRICE: $

NRC FORM 335 (7-77)

UNITED STATES
NUCLEAR REGULATORY COMMISSION
WASHINGTON, D.C. 20555

OFFICIAL BUSINESS

POSTAGE & FEES PAID
U.S. Nuclear Regulatory Commission

U.S.MAIL